## REVIEW ARTICLE

# Substitution reactions in metal–organic frameworks and metal–organic polyhedra

Yi Han, Jian-Rong Li,* Yabo Xie and Guangsheng Guo*

Substitution reaction, as one of the most powerful and efficient chemical reactions, has been widely used in various syntheses, including those for the design and preparation of functional molecules or materials. In the past decade, a class of newly developed inorganic–organic hybrid materials, namely metal–organic materials (MOMs), has experienced a rapid development. MOMs are composed of metal-containing nodes connected by organic linkers through strong chemical bonds, and can be divided into metal–organic frameworks (MOFs) and metal–organic polygons/polyhedra (MOPs) with infinite and discrete structural features, respectively. Recent research has shown that the substitution reaction can be used as a new strategy in the synthesis and modification of MOFs and MOPs, particularly for pre-designed ones with desired structures and functions, which are usually difficult to access by a direct one-pot self-assembly synthetic approach. This review highlights the implementation of the substitution reaction in MOFs and MOPs. Examples of substitution reactions at metal ions, organic ligands, and free guest molecules of MOFs and MOPs are listed and analyzed. The changes or modifications in the structures and/or properties of these materials induced by the substitutions, as well as the nature of the associated reaction, are discussed, with the conclusion that the substitution reaction is really feasible and powerful in synthesizing and tailoring MOMs.

## 1. Introduction

Solid-state materials chemically composed of inorganic,[1–3] organic,[4,5] and inorganic–organic hybrid species[6,7] play an

*Department of Chemistry and Chemical Engineering, College of Environmental and Energy Engineering, Beijing University of Technology, Beijing 100124, P. R. China. E-mail: jrli@bjut.edu.cn, guogs@bjut.edu.cn*

important role in every aspect of our daily life and in industrial manufacture. In the recent decade, as a novel class of inorganic–organic hybrid materials, metal–organic materials (MOMs)[8–11] have experienced a rapid development due to their diverse and easily tailored structures and associated properties, as well as potential applications[12,13] such as in gas storage,[14,15] separation,[16–20] catalysis,[21–23] chemical sensing,[24–26] and drug delivery.[27–29] MOMs are composed of metal ions or clusters connected by

*Yi Han obtained his PhD degree in 2013 from Zhengzhou University in the research field of small molecule sensing. Then, he joined Prof. Jian-Rong Li's group as a postdoctoral research associate at the Beijing University of Technology. His recent research focuses on the design, synthesis, and application of new porous materials.*

**Yi Han**

*Jian-Rong "Jeff" Li obtained his PhD in 2005 from Nankai University. Until 2007, he was an assistant professor at the same university. In 2004, he was also a research assistant at the Hong Kong University of Science & Technology. From 2008 to 2009, he was a postdoctoral research associate, first at Miami University and later at Texas A&M University; from 2010 he worked as an assistant research scientist at the same*

**Jian-Rong Li**

*university. Since 2011, he has been a full professor at the Beijing University of Technology. His research interest focuses on new porous materials for energy and environmental science.*

organic ligands through strong chemical bonds. This derivative greatly extended the research field of solid-state chemistry and materials science. Two main branches can be derived from MOMs based on their structural features: infinite networked metal–organic frameworks (MOFs) and discrete molecular coordination assemblies;[10,30] the latter in this review primarily refers to metal–organic polygons/polyhedra (MOPs). MOFs and MOPs are mainly made up of metal-based nodes and bridging organic linkers in their host skeletons; however they are also usually associated with guest molecules of coordinated or free species.

So far, the generally used method for the synthesis of MOFs and MOPs is based on the direct reaction of metal ions and organic ligands in a specific solvent system[31] (or in the solid state in a few cases[32]), typically a self-assembly reaction process. This traditional synthetic route is quite convenient and dominant, but limited to some extent. Normally, metal ions possess variational coordination geometries in different coordination cases, for example, the $Cu^{2+}$ ion can adopt octahedral, square pyramidal, square-planar, or trigonal bi-pyramidal configurations and $Zn^{2+}$ prefers octahedral or tetrahedral configurations. Similarly, organic ligands such as carboxylic species possess a variety of coordination modes under different reaction/coordination conditions. Furthermore, the coordination or combination of given metal ions and organic ligands can also be affected by some other factors, including reaction temperature, reactant concentration, solvents used, template, and so on,[33–38] thereby resulting in distinct outcomes. That means, it is difficult to find a suitable reaction condition to control the outcome of such a self-assembly process in some cases, particularly when using a new type of ligand to synthesize MOPs or MOFs. However, it should clarify that even so, we agree upon the easy control and modification of MOFs and MOPs in the synthesis, which emphasizes mostly the outcomes from the reaction between metal ions and ligands under a given/optimized synthetic condition.[39,40]

Alternately, the substitution reaction, as one of the most powerful and efficient chemical reactions, has been widely used in inorganic and organic chemistry, particularly for designing and preparing functional molecules.[41–43] A straightforward definition of substitution reaction is that it is a reaction in which any atom or group in a molecule is replaced by another atom or group. The overall substitution reaction can be represented as R–L + A → R–A + L, where R–L and A are the reaction substrate and the attacking reagent, respectively, and R–A and L are the substituted product and the leaving group, respectively. Recent research has indeed shown that the substitution reaction can be used as a new strategy for the synthesis and modification of MOFs and MOPs, particularly for pre-designed ones with desired structures and functions, when a direct self-assembly approach is not able to give the expected product.[44–47] In this context, the substitution reaction usually takes place via a two-phase process and it can be divided into three types: (1) two kinds of solid MOMs are mixed together and suspended in a specific solvent (sometimes a solvent is not required) for a given period of time to achieve the reaction, known as a solid–solid substitution process; (2) one solid MOM is soaked in a solution containing the attacking metal ions, organic ligands, or guest molecules to get substituted MOM, known as a solid–liquid substitution process, being extensively adopted in MOFs; (3) a soluble MOP is reacted with new organic ligands or metal ions in given solvents to get new MOPs or MOFs, known as a liquid–liquid substitution process.

Because of the simple operation and mild reaction conditions, the substitution reaction has been increasingly identified as a new synthetic strategy towards arriving at expected and desired MOMs. In such a substitution process the parent MOM can be regarded as a template to fabricate a new MOM, which greatly enhances the controllability of the resulting MOM in terms of both its structure and property. In addition, with the control of reactant concentration and/or reaction time, different substitution degrees can be easily achieved to get partially or



**Yabo Xie**

*Yabo Xie obtained his PhD in 2004 from Nankai University. From 1991 to 2001, he was a lecturer at Hebei Normal University. From 2005, he was an assistant professor and then associate professor at the Beijing University of Technology. His research interest focuses on the design, synthesis, and property exploration of coordination polymers, and crystal engineering.*



**Guangsheng Guo**

*Guangsheng Guo obtained his PhD from the Beijing University of Chemical Technology. From 1986 to 2009, he was an assistant professor, associate professor, and professor at the same university. In 1995, he was also a visiting scholar at the Chinese University of Hong Kong, where he conducted profound research in the field of Higher Education. Since 2010, he has been a full professor at the Beijing University of Technology.*

*His research interest focuses on the preparation and application of nano-functional materials and applied laser-chemistry, as well as higher education management.*

completely substituted products. Particularly, the partially substituted product is thus multi-component, which usually presents unique multi-functionalities. Furthermore, when several reactants are used, more complicated multi-component substituted MOMs might also be obtained, which would present interesting multi-functionalities.

Whether it is partial or complete substitution, these reactions usually involve the cleavage and regeneration of coordination bonds between metal ions and organic ligands. The partial substitution of a framework often maintains its original network skeleton, while a complete substitution can lead to structural transformation accompanied by changes in the coordination environment, framework dimensionality, and structural inter-penetration. Besides structural modifications, the performance of the final materials in terms of their properties and functions can be improved through the substitutions. For example, substitution at the central metal ion can make the parent inert material catalytically more active, modify its magnetic properties, or change its gas storage/separation capacity; substitution at the organic ligand can desirably tune pore size or surface functionality; and substitution at the free guest molecule can finely modulate fluorescence performance and molecule sorption. In this context, the substitution reaction has indeed been proposed to be an ideal and feasible approach for the synthesis and modification of properties of solid materials.

The substitutions of metal ions and/or ligands in the network skeletons of MOMs were firstly observed in less chemically stable materials where metal–ligand coordination bonds were com-paratively labile, but recently they were also observed in some highly robust systems.[48–51] The mechanism involved in the reactions is obviously important. Cohen and co-workers demon-strated that the central metal ion or organic bridging ligand substitution in MOFs should be an absolute substitution process due to the reversible nature of the coordination bond, suggesting that the substitution was almost widespread in MOMs.[48] Even so, it should be pointed out that the substitution in some highly stable MOMs is quite difficult due to the strong bonds between metal ions and organic ligands. For example, MIL-101(Cr)[52] is a chemically stable MOF, and attempts to exchange the metal ion or the organic ligand in it failed.[48]

In some cases, before and after substitutions, the samples of MOMs are still crystalline, particularly for MOFs; single-crystal X-ray diffraction (SXRD) and powder X-ray diffraction (PXRD) are thus principal methods for characterizing the resulting substituted materials. In addition, aerosol time-of-flight mass spectroscopy (ATOFMS) has also been applied to analyze the chemical composition of microcrystalline particles of sub-stituted MOFs in this topic. Other characterization methods such as $^1$H NMR, UV-Vis, field emission scanning electron microscopy (FE-SEM), energy dispersive X-ray spectrometry (EDS), and time-dependent DFT calculations can also be used in these related studies.

Clearly, substitution reaction is a promising and feasible approach in the design and preparation of novel MOMs that may be difficult to access by other synthetic methods. Although several excellent reviews on the topics of metal

exchange/transmetalation,[44,45] sequential self-assembly,[46] solid-state reactivity,[47,53] single-crystal to single-crystal (SC–SC) transformation,[54,55] and post-synthetic modification (PSM) in MOFs[56–59] have recently appeared, a review for the summing-up and understanding of the substitution reactions in MOMs is still lacking. Herein, we attempt to collect and comment upon reported examples from our and others' work to contribute a review article on this new topic of substitution reaction in MOFs and MOPs. The discussions are organized based on the following three aspects: substitution at metal ions, substitution at organic ligands, and substitution at free guest molecules.

## 2. Substitution at metal ions

Single metal ions as the inorganic moieties predominated in the early stage of MOM development. Subsequently, an important evolution was of using metal clusters, usually called secondary building units (SBUs), to generate porous MOMs, which could enhance the robustness and structural controllability of the resulting materials.[39,60–62] The metal containing entities as the essential part of MOMs mainly include central metal ions/ clusters and metal ions within some metalloligands. Moreover, coordinated guest molecules on metal moieties can also be replaced by other chemical entities; thus we consider these three types of related substitutions under the same class, as the substitution at metal ions.

### 2.1. Central metal ion substitution

Since a MOM is essentially the metal salt of a base (such as pyridine-based ligand) or a conjugate base of a weak acid (such as carboxylate ligand), the substitution of the original metal ion in the backbone of a MOF or MOP by other metal ions, retaining the integrality of the framework, should be feasible based on an acid–base displacement reaction. Central metal ion substitution (also called central metal exchange,[63,64] trans-metalation,[44,45] or postsynthetic cation exchange,[48] in some cases) has indeed undergone a rapid development in the last few years, and has become a feasible method for the functional modification of MOFs. By introducing suitable metal ions into well-defined structures, central metal ion substitution enables the rational design and control of physical and chemical properties of the resulting materials. Some examples have demonstrated the complete or partial substitution of metal centers in MOFs performed under mild conditions, and accompanied by changes in the related properties.

Long and co-workers have reported one of the earliest examples of metal ion substitution in MOFs.[65] They presented the central metal substitution in the MOF, {Mn$_3$[(Mn$_4$Cl)$_3$(BTT)$_8$(CH$_3$OH)$_{10}$]$_2$}$_n$ (BTT = 1,3,5-benzenetristetrazolate), with a sod network topology, in which chloride-centered square-planar [Mn$_4$Cl]$^{7+}$ units are linked by BTT$^{3-}$ ligands to form an anionic three-dimensional (3D) framework, while the charge is balanced by Mn$^{2+}$ solvates.[66] As shown in Fig. 1, the substitution of Mn$^{2+}$ ions in both the framework backbones and/or the cations with selected mono-valent and divalent ions including Li$^+$, Cu$^+$, Fe$^{2+}$, Co$^{2+}$, Ni$^{2+}$, Cu$^{2+}$,
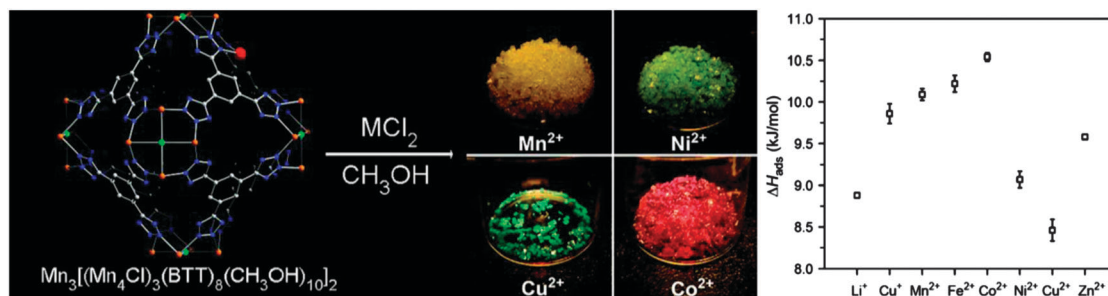
5954 | *Chem. Soc. Rev.*, 2014, **43**, 5952–5981

This journal is © The Royal Society of Chemistry 2014

Fig. 1 The substitution of $Mn^{2+}$ ions in $\{Mn_3[(Mn_4Cl)_3(BTT)_8(CH_3OH)_{10}]_2\}_n$ with selected metal ions results in the formation of isostructural substituted materials (left). The enthalpies of $H_2$ adsorption in the original and substituted MOFs (right). Reprinted with permission from ref. 65. Copyright 2007 American Chemical Society.

and $Zn^{2+}$ resulted in the formation of a series of isostructural MOFs with different colors. Inductively coupled plasma-atomic absorption (ICP-AA) measurements demonstrated that along with the expected substitution of extra-framework $Mn^{2+}$ ions, the adsorption of metal halides took place in the $Fe^{2+}$ or $Co^{2+}$ solution, to form $\{Fe_3[(Mn_4Cl)_3(BTT)_8]_2 \cdot FeCl_2\}_n$ and $\{Co_3[(Mn_4Cl)_3-(BTT)_8]_2 \cdot 1.7CoCl_2\}_n$, respectively. However, for the $Cu^{2+}$ or $Zn^{2+}$ substitution, a significant degree of intra-framework $Mn^{2+}$ ion substitution also occurred simultaneously, to form $\{Cu_3[(Cu_{2.9}-Mn_{1.1}Cl)_3(BTT)_8]_2 \cdot 2CuCl_2\}_n$ and $\{Zn_3[(Zn_{0.7}Mn_{3.3}Cl)_3(BTT)_8]_2 \cdot 2ZnCl_2\}_n$, respectively. For the replacement in this MOF with monovalent ions, only partial substitution of extra-framework $Mn^{2+}$ ions was observed for $Li^+$ to give $\{Li_{3.2}Mn_{1.4}[(Mn_4Cl)_3-(BTT)_8]_2 \cdot 0.4LiCl\}_n$, and almost negligible substitution was observed for $Cu^+$ ions. These results demonstrated that the substitution in this system was metal ion dependent. Subsequent $H_2$ sorption experiments revealed the variation of adsorption enthalpies among these metal-substituted MOFs, indicating a dependence of the $H_2$ binding strength on the nature of the metal ions. It was found that $Fe^{2+}$ and $Co^{2+}$ ion substituted MOFs exhibited stronger $H_2$ binding than the parent material, with the $Co^{2+}$ substituted MOF having the highest initial adsorption enthalpy of 10.5 kJ mol$^{-1}$.

Similarly, Hou and co-workers also confirmed that the central metal ion substitution took place along with metal ion sorption when a series of ferrocenyl carboxylate MOF samples were immersed in the aqueous solution of target metal ions.[67–69] Interestingly, it was found that central metal ion substitution occurred in single crystals, whereas the MOF crystals grinded into powder showed metal ion sorption. And, the metal ion sorption mainly occurred in a dilute solution system, while both the substitution and sorption dominated in a concentrated solution. Moreover, they also found that the substitution rate of metal ions was higher in low-dimensional structure MOFs than in high-dimensional structure MOFs, likely owing to high steric hindrance in the latter.

They observed the central metal ion substitution not only in MOF, but also in a MOP, $[Cu_8L_{16}]$ (HL = 4′-4-methyl-6-(1-methyl-1$H$-benzimidazolyl-2-group)-2-$n$-propyl-1$H$-benzimidazolyl methyl), which has a double-helical wheel structure (Fig. 2).[70] In the structure the central $Cu^{2+}$ ion has a slightly distorted quadrilateral coordination geometry, which gives more room for accepting the incoming metal ions, thereby helping the observed substitution.
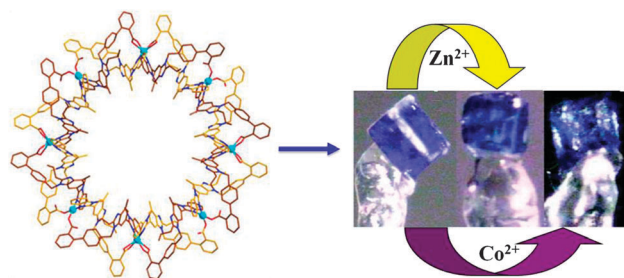


Fig. 2 Double-helical octanuclear wheel structure of $[Cu_8L_{16}]$ (left). Single crystal photos of $[Cu_8L_{16}]$, $Zn^{2+}$-, and $Co^{2+}$-substituted analogues (right). Reprinted with permission from ref. 70. Copyright 2008 American Chemical Society.

By immersing the crystals of this MOP in an aqueous solution of $Zn^{2+}$ or $Co^{2+}$ ions for 5 days, the partially substituted crystals of $[Zn_{1.6}Cu_{6.4}L_{16}]$ and $[Co_{1.2}Cu_{6.8}L_{16}]$ were harvested, respectively. SXRD and PXRD analyses confirmed the occurrence of the reactions, and showed that the process in both cases was a SC–SC transformation induced by the central metal ion substitution. Furthermore, they also demonstrated that the central metal ion substitution reaction was indeed related to the coordination ability of the incoming metal ions towards the organic ligands. When the coordination ability of the incoming metal ions was close to that of the original metal ion, the substitution occurred and the resulting products preserved the original structure. It was also found that these MOP materials with different substituted metal ions presented different antitumor properties and $H_2$ uptake capacities.

Another example of the central metal ion substitution was reported by Zhao and co-workers.[71] They achieved the substitution of $Zn^{2+}$ by $Cu^{2+}$ ions in a 3D structural MOF, $[Zn_2(L)(DMF)_3]_n$ (NTU-101-Zn; L = 5,5′-(1$H$-1,2,3-triazole-1,4-diyl)-diisophthalate, DMF = $N,N$-dimethylformamide) (Fig. 3). In this MOF, there exist two crystallographically independent $Zn^{2+}$ ions with one coordinating with three DMF molecules, which perhaps makes it easily accessible and replaceable by other metal ions. When the crystals of NTU-101-Zn were soaked in a DMF solution of $Cu(NO_3)_2$ for two weeks, the original colorless crystals gradually turned into green-blue ones (NTU-101-Cu) while maintaining their original shapes and sizes and thereby the same framework structure as confirmed by PXRD. Inductively coupled plasma

This journal is © The Royal Society of Chemistry 2014

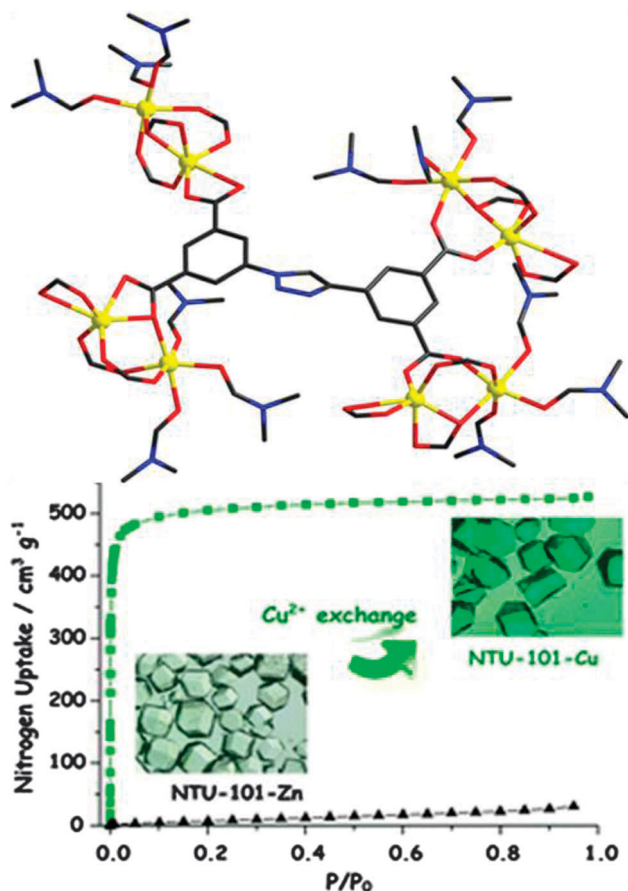Chem. Soc. Rev., 2014, 43, 5952–5981 | 5955

Fig. 3 Crystal structure of NTU-101-Zn showing coordination environments of organic ligands and metal ions (top). Color change along with the metal ion substitution and N₂ sorption isotherms of activated NTU-101-Zn and NTU-101-Cu at 77 K (bottom). Reprinted with permission from ref. 71. Copyright 2012 The Royal Society of Chemistry.
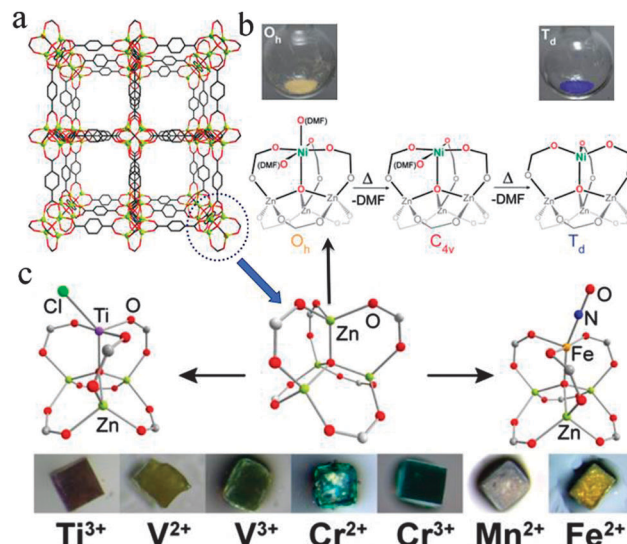


Fig. 4 (a) Crystal structure of MOF-5. (b) Color change accompanied by the sequential loss of DMF molecules from the $(DMF)_2NiZn_3O(COO)_6$ cluster. (c) The $MZn_3O(COO)_6$ cluster featuring $Ti^{3+}$ and $Fe^{2+}$ substitutions and crystal photos of all metal-substituted MOF-5 analogues. Reprinted with permission from ref. 73 and 76. Copyright 2012 The Royal Society of Chemistry and 2013 American Chemical Society.

(ICP) analysis indicated that approximately 80% of $Zn^{2+}$ ions were substituted by $Cu^{2+}$ ions in this process, and there was no significant increase in substitution with the extension of the reaction time. They also demonstrated that the substitution process was irreversible, by putting NTU-101-Cu in a concentrated DMF solution of $Zn(NO_3)_2$ for a long period of time. This result suggested that the framework of NTU-101-Cu was more stable than that of NTU-101-Zn, which was also confirmed by subsequent gas adsorption experiments. It was found that the activated NTU-101-Cu exhibited a $N_2$ adsorption uptake of 526 cm³ g⁻¹ at 1 atm and a higher adsorption selectivity towards $CO_2$ over $N_2$ and $CH_4$, whereas the framework of NTU-101-Zn collapsed upon sample activation as evidenced by PXRD, resulting in poor gas adsorption capacities towards both $N_2$ and $CO_2$.

Similarly, Cheng and co-workers reported the substitution of $Zn^{2+}$ ions by $Cu^{2+}$, $Co^{2+}$, and $Ni^{2+}$ ions in MOF $\{[Zn_7(L)_3(H_2O)_7]\cdot[Zn_5(L)_3(H_2O)_5]\}_n$ (L = N-phenyl-N'-phenyl bicyclo[2,2,2]oct-7-ene-2,3,5,6-tetracarboxdiimide tetracarboxylate), which was built by interpenetrated cationic $[Zn_7(L)_3(H_2O)_7]$ (MOF-A⁺) and anionic $[Zn_5(L)_3(H_2O)_5]$ (MOF-B⁻) networks.[72] The crystals of this MOF were immersed in a methanol solution of $Cu^{2+}$, $Co^{2+}$, or $Ni^{2+}$ ions for one week to achieve the metal ion substitution.

It was found that approximately 87% of the $Zn^{2+}$ was substituted by $Cu^{2+}$ ions, while $Co^{2+}$ or $Ni^{2+}$ ions were not detected in the resulting respective material. PXRD confirmed that the resulting Cu-substituted MOF was isostructural with the original one. The authors attributed the substitution only with $Cu^{2+}$ to the fact that $Cu^{2+}$ and $Zn^{2+}$ ions have almost similar ionic diameter and coordination geometry or feature.

In the examples discussed above a partial substitution of central metal ions was observed. The authors did not explore why a complete substitution did not occur in the target samples, or the exact location of the substituted metal ions in a MOF with multiple crystallographically independent central metal sites. This information would be very useful in elucidating the mechanism involved in these substitution reactions. In this context, Dincă and co-workers proposed that a kinetic barrier induced by the preferential coordination geometries of metal ions indeed dominated the partial or complete substitution.[73] They initiated the study of the substitution of $Zn^{2+}$ ions with $Ni^{2+}$ ions in the $Zn_4O$ cluster of $[Zn_4O(BDC)_3]_n$ (MOF-5; BDC = 1,4-benzenedicarboxylate) (Fig. 4a and b).[60] By soaking colorless crystals of MOF-5 in a saturated DMF solution of $Ni(NO_3)_2$ for 1 year, a Zn : Ni ratio of 3 : 1 in the $[M_4O]^{6+}$ cluster of the resulting yellow crystals was achieved. This limited content of $Ni^{2+}$ in the final material was consistent with the results observed in the earlier reported Co- and Ni-doped MOF-5 materials synthesized by a direct reaction of different Zn : Ni/Co ratio (up to 1 : 6) metal salts with the ligand.[74,75] Based on the fact that the $Ni^{2+}$ ion prefers an octahedral coordination in the oxygen ligand field, the authors attributed the observed phenomenon to the fact that an octahedrally coordinated $Ni^{2+}$ ion distorted the parent $Zn_4O$ core and the framework lattice, which prevented the incorporation of additional $Ni^{2+}$ ions due to the presence of

a large kinetic barrier. In addition, thermogravimetric analysis (TGA) confirmed that two DMF molecules coordinated to each $Ni^{2+}$ center in the substituted structure. Heating the Ni-substituted MOF-5 led to a color change from yellow to blue-purple, implying that a pseudo-tetrahedral $Ni^{2+}$ ion might be generated. $N_2$ absorption analysis indicated that this blue Ni-MOF-5 material had a $N_2$ uptake of 825 cm$^3$ at 1 atm and 77 K and a BET surface area of 3300 (100) m$^2$ g$^{-1}$, which were very close to those of the parent MOF-5. In the following work, this group prepared redox-active $Ti^{3+}$-, $V^{2+/3+}$-, $Cr^{2+/3+}$-, $Mn^{2+}$-, and $Fe^{2+}$-substituted MOF-5 materials by soaking MOF-5 crystals in a concentrated DMF solution of $TiCl_3 \cdot 3THF$, $VCl_2$(pyridine)$_4$, $VCl_3 \cdot 3THF$, $CrCl_2$, $CrCl_3 \cdot 3THF$, $MnCl_2$, or $Fe(BF_4)_2 \cdot 6H_2O$ for one week (Fig. 4c).[76] Unlike Ni-MOF-5, this series of substituted MOF-5 materials cannot be obtained by a direct solvothermal reaction of the starting reactants of $Zn(NO_3)_2$ with the corresponding metal ion sources. Importantly, it was found that the substitution rates of metal ions in these cases were much faster than that observed in the $Ni^{2+}$ ion case, and the substitution degrees seemed to be kinetically controlled by the stability constant of each substituting metal ion. Furthermore, all these MOF-5 substituents were highly porous with BET surface areas ranging from 2393 m$^2$ g$^{-1}$ to 2700 m$^2$ g$^{-1}$, which were lower than that of Ni-MOF-5 (3300 m$^2$ g$^{-1}$). They attributed this to a partial disruption and introduction of defects in the MOF lattice by the rapid substitution.

On the other hand, Dincă and co-workers demonstrated that multi-wavelength anomalous dispersion (MAD) was a powerful technique to determine the locations of substituted metal ions in MOFs with more than one crystallographically independent metal site.[77] By treating colorless crystals of MOF $\{Mn_3[(Mn_4Cl)_3(BTT)_8]_2\}_n$ (MnMnBTT) with a concentrated solution of $Fe^{2+}$, $Zn^{2+}$, or $Cu^{2+}$ ions in MeOH for 7 days, followed by heating under dynamic vacuum for 12 hours at 150 °C, they obtained FeMnBTT, CuMnBTT, and ZnMnBTT materials, respectively. The MAD analyses demonstrated that only the extra-framework $Mn^{2+}$ ions were substituted. It was also found that upon removal of solvent molecules dissociative metal ions in the original or substituted frameworks migrated to bind the tetrazolyl N atoms of the ligands, and simultaneously free water molecules inside the cavities also bound to these metal ions.

Similar partial substitution controlled by the preferential coordination of metal ions was also observed in MOF $[Zn_5Cl_4(BTDD)_3]_n$ (MFU-4l; $H_2BTDD$ = bis(1H-1,2,3-triazolo-[4,5-b], [4',5'-i])dibenzo-[1,4]-dioxin)[78] reported by Volkmer and co-workers.[79] There are two crystallographically independent $Zn^{2+}$ ions in the MOF structures: one is octahedral and the other is tetrahedral. It was found that heating MFU-4l in a DMF solution of $Co^{2+}$ ions led to the replacement of only tetrahedral $Zn^{2+}$ centers, whereas the octahedral ones remained intact. Interestingly, an attempt at $Co^{2+}$ substitution in a MOF of similar structure $\{[Zn_5Cl_4(BBTA)_3] \cdot 3DMF\}_n$ (MFU-4; $H_2BBTA$ = 1H,5H-benzo(1,2-d:4,5-d')bistriazole)[80] was unsuccessful probably due to the diffusion limitation from small pores in this MOF structure.[79] Therefore, the presence of larger pores in the MOF seems to be a prerequisite for the metal ion substitution

in this system. In addition, the metal ion substitution in MFU-4l had introduced unsaturated tetrahedral $Co^{2+}$ centers into the resulting material, which efficaciously enhanced its catalytic activity towards CO oxidation.

It is clear that apart from the coordination bond features, the coordination geometries of metal ions, steric hindrance, kinetic barrier, and pore sizes of MOFs also play key roles in deciding the degree of central metal ion substitutions, as demonstrated by the above examples of partial substitutions. To achieve a high degree of substitution or complete substitution, all these factors should be considered. One straightforward strategy is to use MOFs with large pores and substituted metal ions having similar properties.

Kim and co-workers reported the complete substitution of central metal ions in the MOF $\{Cd_{1.5}[H_3O]_3[(Cd_4O)_3(HETT)_8] \cdot 6H_2O\}_n$ (HETT = 5,5',10,10',15,15'-hexaethyltruxene-2,7,12-tricarboxylate) (Fig. 5, top).[81] When crystals of this MOF were immersed in an aqueous solution of $Pb^{2+}$ ions, almost 98% of $Cd^{2+}$ ions from the framework were replaced by $Pb^{2+}$ ions within 2 hours and a complete substitution was achieved in 2 days, as confirmed by inductively coupled plasma atomic emission spectroscopy (ICP-AES), to give the $Pb^{2+}$-substituted MOF. The authors also confirmed that the exchange process was reversible, but the reverse process took a longer time. The ICP-AES analysis showed that about 50% $Pb^{2+}$ were replaced by $Cd^{2+}$ in 1 day, and the exchange completed in almost 3 weeks. This complete reversible substitution was also a SC–SC transformation process, as evidenced by SXRD analysis. Furthermore, $Cd^{2+}$ ions in this MOF could also be completely substituted by lanthanide ions such as $Nd^{3+}$ and $Dy^{3+}$ in a longer time of 12 days. It was also noted that the syntheses of
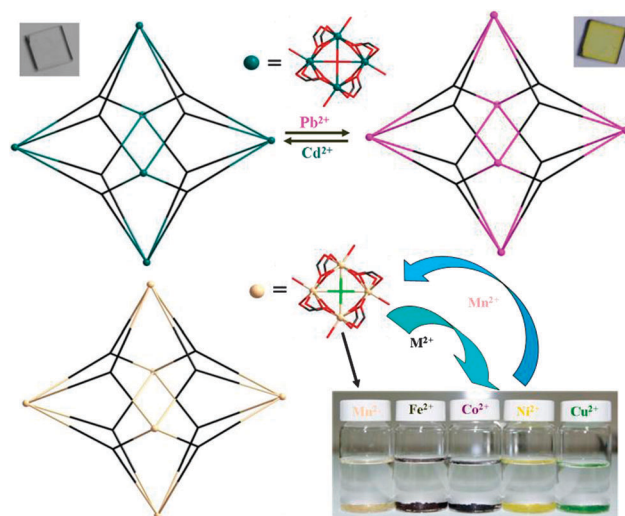


Fig. 5 Reversible and complete central metal ion substitution in the $[Cd_4O]^{6+}$ unit of $\{Cd_{1.5}[H_3O]_3[(Cd_4O)_3(HETT)_8] \cdot 6H_2O\}_n$ (top). Syntheses of POST-65-M (M = $Fe^{2+}$, $Co^{2+}$, $Ni^{2+}$, or $Cu^{2+}$) through the metal ion substitution in $\{Mn[H_3O][(Mn_4Cl)_3(HMTT)_8]\}_n$ (POST-65) and the reversible return (bottom). Reprinted with permission from ref. 81 and 82. Copyright 2009 American Chemical Society and 2012 WILEY-VCH Verlag GmbH & Co. KGaA, Weinheim.

This journal is © The Royal Society of Chemistry 2014

Chem. Soc. Rev., 2014, 43, 5952–5981 | 5957

the two Ln-MOFs were indeed quite difficult based on the direct reaction between lanthanide ions and the $H_3HETT$ ligand. SXRD analysis of the Dy-MOF revealed a hydroxyl-bridged square planar $\{Dy_4(\mu_4\text{-}OH)\}^{11+}$ instead of $\{Cd_4(\mu_4\text{-}O)\}^{6+}$ unit in its structure, but the original framework topology was still preserved.

Shortly afterwards, another complete and reversible metal ion substitution was demonstrated in a MOF of similar structure $\{Mn[H_3O][(Mn_4Cl)_3(HMTT)_8]\}_n$ (POST-65; HMTT = 5,5′,10,10′,15,15′-hexamethyltruxene-2,7,12-tricarboxylate) by the same group (Fig. 5, bottom).[82] Soaking the POST-65 in DMF solutions of $MCl_2$ (M = $Fe^{2+}$, $Co^{2+}$, $Ni^{2+}$, or $Cu^{2+}$) for 12 days led to the formation of POST-65(Fe/Co/Ni/Cu) with preserved framework structures, which were indeed difficult to access by the direct reaction between the respective metal salt and the ligand. It was also confirmed that POST-65(Fe) had a different SBU of $\{Fe_4OH\}^{11+}$ compared to that in the parent and other substituted MOF-65, going with the observation of $Fe^{3+}$ rather than $Fe^{2+}$ in it. In addition, $H_2$ adsorption and magnetization measurements demonstrated the metal-specific properties of these POST-65 MOFs. Different from these, a complete but irreversible central metal ion substitution by $Co^{2+}$ and $Ni^{2+}$ ions in $\{Cd_3[(Cd_4Cl)_3(BTT)_8]_2\}_n$ was observed by Liao and co-workers.[83] Gas adsorption studies showed that the resulting two substituted products exhibited larger adsorption capacities than the parent.

Similarly, Zou and co-workers tested the possibility of complete metal ion substitution in paddle-wheel SBU-based MOF systems.[84] In a mesoporous MOF $\{[Zn_6(BTB)_4(BIPY)_3]\cdot(S)_x\}_n$ (SUMOF-1-Zn; $H_3BTB$ = 4,4′,4″-benzene-1,3,5-triylbenzoic acid; BIPY = 4,4′-bipyridine; S = solvent molecules), it was found that the $Zn^{2+}$ ions in the paddle-wheel SBUs could be substituted by other transition metal ions including $Co^{2+}$, $Ni^{2+}$, and $Cu^{2+}$ via a SC–SC transformation. The kinetic studies monitored by ICP-AES showed that 50% of the $Zn^{2+}$ ions were replaced by $Cu^{2+}$ ions within 1 hour, 95% within 3 days, and almost complete substitution (99%) was achieved in 3 months. But the $Zn^{2+}$ ions could only be partially exchanged by $Co^{2+}$ and $Ni^{2+}$ ions with a lower substitution rate of 38% and 35%, respectively, even after 3 months. It was also interesting that only 38% of $Cu^{2+}$ ions in SUMOF-1-Cu could be exchanged by $Zn^{2+}$ ions even after 3 months, whereas metal ions in the $Co^{2+}$ and $Ni^{2+}$-based MOFs could be completely substituted by $Zn^{2+}$ ions within only 7 days. The relative stabilities of the dinuclear paddle-wheel $[M_2(O_2C\text{-}R)_4]$ can thus be deduced to be in the order of Co $\approx$ Ni < Zn < Cu, which is consistent with the Irving–Williams series.[85] Complete central metal ion substitutions of other Zn-paddle-wheel based MOFs by $Cu^{2+}$ were also reported by Zhou's[86] and Suh's[87] groups. In Zhou's work, the resulting Cu-substituted MOF exhibited an increased stability and enhanced adsorption ability towards $N_2$, $H_2$, $CO_2$, and $CH_4$. The authors attributed the increased stability to the $Cu^{2+}$ ion having a decreased distorted square pyramidal configuration in the paddle-wheel cluster, as opposed to the $Zn^{2+}$ ion. In addition, it was found that the $Cd^{2+}$ ions in $\{[Cd_6(BPT)_4Cl_4(H_2O)_4]\cdot[C_{44}H_{36}N_8CdCl]\cdot[H_3O]\cdot(S)\}_n$ (porph@MOM-10; BPT = biphenyl-3,4′,5-tricarboxylate) could be completely substituted by $Mn^{2+}$ ions, but only partially replaced by $Cu^{2+}$ ions.[88] The authors
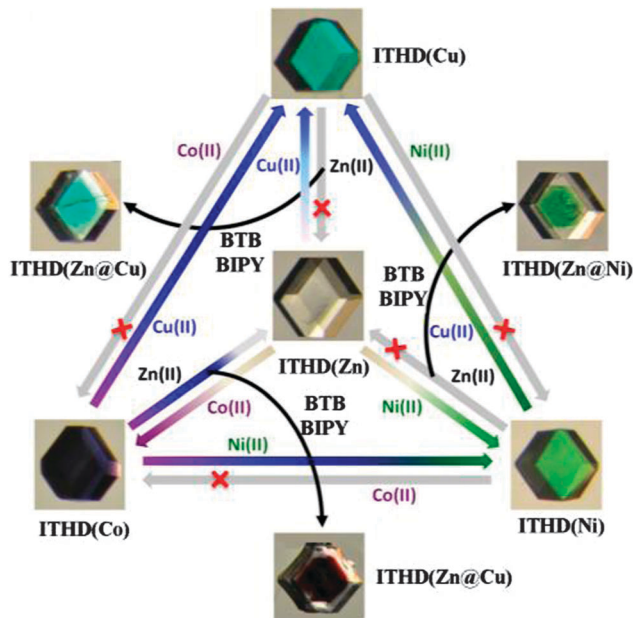


Fig. 6 Schematic representation of central metal ion substitutions and epitaxial growth of core−shell crystals of $[M_6(BTB)_4(BIPY)_3]_n$ (ITHD(M); M = $Zn^{2+}$, $Co^{2+}$, $Cu^{2+}$, and $Ni^{2+}$). Reprinted with permission from ref. 89. Copyright 2012 American Chemical Society.

attributed these observed results to the lability of the high-spin $d^{10}$ and $d^9$ metal ions and the relative inertness of the low-spin $d^5$ $Mn^{2+}$ ion in this system. The resulting porph@MOM-Mn and -Cu materials were permanently porous and exhibited catalytic activity in the epoxidation of trans-stilbene by t-BuOOH.

On the other hand, it was considered that central metal ion substitution usually went forward from the surface to the core in a MOF crystal. It means that MOFs with different substitution degrees can be isolated by the control of the reaction time, leading to some unique core–shell MOF crystals. Lah and co-workers reported the progress of substitution in the crystals of MOFs, $[M_6(BTB)_4(BIPY)_3]_n$ (ITHD(M); M = $Zn^{2+}$, $Co^{2+}$, $Cu^{2+}$, and $Ni^{2+}$), as shown in Fig. 6.[89] The central metal ion substitution experiments were performed by soaking crystals of ITHD(M) MOF in DMF solutions of various metal nitrates. Because it would take time for the metal ions to diffuse from the surface to the core in a crystal, a higher rate was observed at the beginning of the substitution. Thus, both thermodynamically controlled complete substitution and kinetically controlled core–shell heterostructures were finally achieved by controlling the soaking time. Meanwhile, these core–shell crystals could also be prepared by using an epitaxial growth technique as shown in Fig. 6. Similar situations have been observed in $[Zn_3(BTC)_2(H_2O)_2]_n$ (Zn-HKUST-1; BTC = 1,3,5-benzenetricarboxylate) and $[Zn_{24}L_8(H_2O)_{12}]_n$ (PMOF-2; $H_6L$ = 1,2,3-tris(3,5-dicarboxylphenylethynyl)benzene).[90] Except for the formation of core–shell structures/crystals, this work also demonstrated that solvents had a significant effect on the kinetics of the central metal ion substitution: much faster exchange in a MeOH solution of $Cu^{2+}$ ions than in DMF. In addition, $Zn^{2+}$ ions in Zn-HKUST-1 could only be partially substituted by $Cu^{2+}$ even after 3 months, whereas PMOF-2 underwent a complete substitution in
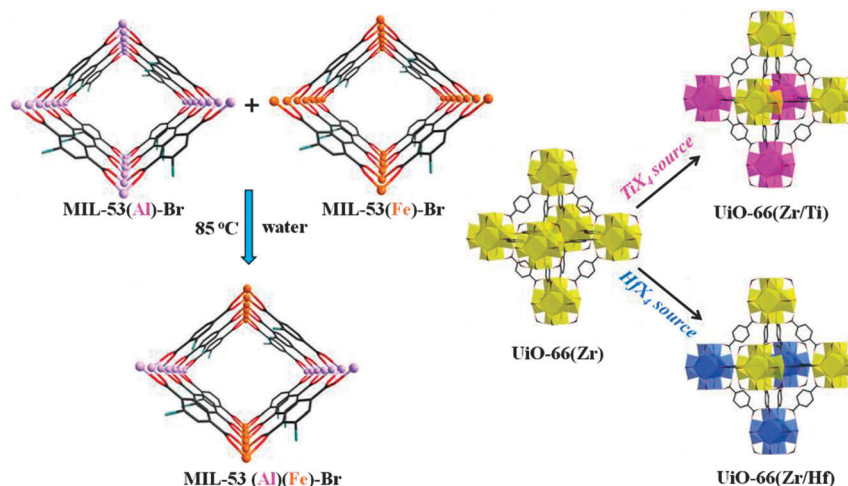
5958 | Chem. Soc. Rev., 2014, 43, 5952–5981

This journal is © The Royal Society of Chemistry 2014

**Fig. 7** Central metal ion substitutions in $[M(OH)(BDC-Br)]_n$ (MIL-53 series; M = $Al^{3+}$ or $Fe^{3+}$) (left)[48] and $[M_6O_4(OH)_4(BDC)_6]_n$ (UiO-66 series; M = $Zr^{4+}$, $Ti^{4+}$ or $Hf^{4+}$) (right).[94]

just 3 days. The authors attributed this difference to the much more flexibility of the ligand L compared to BTC. These findings not only demonstrate that the solvent selection is important for the metal ion substitution which is usually controlled by kinetics, but also clarify possible factors triggering a thermodynamically controlled complete substitution, including the sizes, shapes, and properties of the linkers and the framework structures.

In the above-mentioned examples, central metal ion substitutions were observed in some MOFs with low water and thermal stability; however practical applications would require that MOFs possess high stability. Fortunately, water and thermally stable MOFs, such as MIL series,[52,91–93] UiO series,[94] and ZIFs,[95–97] have also been explored for their central metal ion substitution. Cohen and co-workers studied the metal ion exchange[48] between MOFs $[Al(OH)(BDC-Br)]_n$ (MIL-53-Br(Al))[98] and $[Fe(OH)(BDC-Br)]_n$ (MIL-53-Br(Fe)).[99] As shown in Fig. 7 (left), both MOFs were mixed in the solid state and then soaked in water for 5 days at 85 °C. PXRD confirmed that the framework structures of the two MOFs did not change. Aerosol time-of-flight mass spectrometry (ATOFMS) spectra of the resulting solid mixture showed that about 40% of the crystalline particles contained both Al and Fe ions. It was also detected that the particle size did not change, which ruled out the simple mechanical aggregation of the two MOFs. Both characterizations thus suggested the formation of MIL-53-Br(Al/Fe) MOF. They also studied the metal ion substitution in another stable MOF $[Zr_6O_4(OH)_4(BDC)_6]_n$ (UiO-66(Zr)) (Fig. 7, right).[94] After soaking UiO-66(Zr) in the DMF solution of a $Ti^{4+}$ salt, such as $TiCp_2Cl_2$, $TiCl_4(THF)_2$, or $TiBr_4$ (Cp = $\eta^5$-cyclopentadienyl, THF = tetrahydrofuran), for 5 days at 85 °C, it was found that $Zr^{4+}$ ions in the MOF were partially replaced by $Ti^{4+}$ ions, and the Ti-exchange degree was dependent on the metal sources used. $TiBr_4$ showed the lowest exchange level, whereas $TiCl_4(THF)_4$ presented the best with about 38% of metal ions being substituted in the whole sample. A similar experiment was performed with $HfCl_4$, but only a modest amount of $Hf^{4+}$ ions of about 20% was introduced into the UiO-66 MOF even at

an enhanced reaction temperature. It should be pointed out that $Ti^{4+}$ is receiving increasing attention due to its low toxicity, good redox activity, high photocatalytic properties, and lower density in constructing MOFs. However, because of the facile hydrolysis of $Ti^{4+}$ ions, the synthesis of Ti-MOFs is quite challenging with very few examples being reported so far.[100,101] As demonstrated by this work, the metal ion substitution method would thus be feasible and powerful in the preparation of Ti-based MOFs.

ZIFs, mostly based on $Zn^{2+}$ or $Co^{2+}$ ions and combined with inorganic zeotype topologies and organic functionalities, are another subclass of highly stable MOFs. Cohen and co-workers also studied the central metal ion substitution in these MOFs.[49] Activated $[Zn(DCIM)_2]_n$ (ZIF-71; DCIM = 4,5-dichloroimidazole)[102] or $[Zn(MeIM)_2]_n$ (ZIF-8; MeIM = 2-methylimidazolate)[97] was incubated in a MeOH solution of $Mn(ACAC)_2$ (ACAC = acetylacetonate) at 55 °C for 24 hours. X-ray fluorescence spectroscopy (XRF) analysis indicated that about 12% and 10% of the $Zn^{2+}$ ions in them were replaced by $Mn^{2+}$ ions, respectively. Subsequently, exposing ZIF-71(Zn/Mn) to a 3 molar excess of $Zn(ACAC)_2$ solution in MeOH resulted in almost all of $Mn^{2+}$ ions being exchanged by $Zn^{2+}$. These results showed that the central metal ion substitution was indeed a general phenomenon in even very robust MOFs, and the crystallinity and porosity of MOFs could perfectly be inherited in the substitution process. It is also noteworthy that many of the above-mentioned cases underwent partial substitutions but not complete ones, which might be attributed to the strong coordination bonds in these stable MOFs.

As discussed above, in most cases the central metal ion substitution enabled the resulting MOFs to inherit their original framework integrity including the SBUs and the whole structural topologies. However, Zaworotko and co-workers showed that $Cd^{2+}$ ions in $\{[Cd_4(BPT)_4][Cd(C_{44}H_{36}N_8)(S)]\}_n$ (P11) could be completely but irreversibly replaced by $Cu^{2+}$ ions when P11 crystals were immersed in a MeOH solution of $Cu(NO_3)_2$ for 10 days, to form a new MOF of $\{[Cu_8(X)_4(BPT)_4(S)_8](NO_3)_4 \cdot [Cu(C_{44}H_{36}N_8)S] \cdot [S]\}_n$ (P11-Cu) (Fig. 8).[103] SXRD analysis of P11-Cu revealed a new

This journal is © The Royal Society of Chemistry 2014

Chem. Soc. Rev., 2014, **43**, 5952–5981 | **5959**
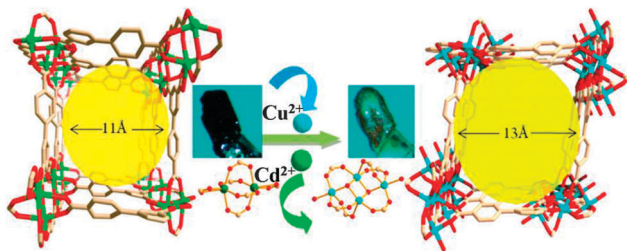
Fig. 8 Schematic representation of the central metal ion substitution in $\{[Cd_4(BPT)_4]-[Cd(C_{44}H_{36}N_8)(S)]\cdot[S]\}_n$ to form $\{[Cu_8(X)_4(BPT)_4(S)_8](NO_3)_4\cdot[Cu(C_{44}H_{36}N_8)S]\cdot[S]\}_n$, accompanied by the generation of tetranuclear $Cu^{2+}$ SBUs from dinuclear $Cd^{2+}$ ones and the modification of pore sizes. Reprinted with permission from ref. 103. Copyright 2013 American Chemical Society.

SBU in its structure and a 20% unit cell volume expansion from 3779.3(2) in P11 to 4133.0(5) $Å^3$. Importantly, P11-Cu afforded a larger pore size and a higher surface area (1406 $m^2$ $g^{-1}$) in comparison to P11 (997 $m^2$ $g^{-1}$). In addition, a stepwise substitution mechanism was proposed in this work. Because the overall linkage geometry of the SBU in P11-Cu is similar to that in P11, the network topologies of P11-Cu and P11 are indeed identical.

## 2.2.  Metal ion substitution within metalloligands

Using metalloligands as building blocks has become a new approach for the construction of functional MOMs.[104] Compared with the central metal ions that usually locate in an environment with larger steric hindrance from ligands, the metal ions in some metalloligands are more open, which is very useful in catalysis and adsorption-based applications.[105–108] For example, in molecular catalysis the metal center within a metalloligand can easily interact with the substrate to display a high activity. Metal ion substitution within the metalloligand is thus a powerful tool for tuning the related properties of MOMs.

A typical metalloligand is metalloporphyrin, which is quite interesting due to its good catalytic activity and molecular binding ability.[109–112] It has been confirmed that some divalent cations in the core of the porphyrin moiety could be easily replaced by others in metalloporphyrins.[113] In MOF systems, Ma and co-workers studied the substitution of the core metal ion in the metalloporphyrin ligand of a MOF called MMPF-5, $\{[Cd_{11}(TDCPP)_3][H_3O]_8\cdot(DMSO)_{36}\cdot(H_2O)_{11}\}_n$ ($H_8TDCPP-H_2$ = tetrakis(3,5-dicarboxyphenyl)porphine; DMSO = dimethyl sulfoxide), which was constructed based on $Cd^{2+}$-metalated tetrakis(3,5-dicarboxyphenyl)porphine (TDCPP-Cd) moieties and triangular $Cd(CO_2)_3$ SBUs.[114,115] Immersing MMPF-5 crystals in a DMSO solution of $Co(NO_3)_2$ at 85 °C for 2 days afforded the $Co^{2+}$-exchanged MMPF-5(Co). UV/Vis spectroscopy studies revealed the complete exchange of $Cd^{2+}$ ions by $Co^{2+}$ ions in the metalloporphyrin ligands. Interestingly, the $Cd^{2+}$ ions in the SBUs of the framework remained intact, possibly due to their strong coordination with O atoms of carboxylate groups. The metal ion substitution in this case is thus selective, with a preference for the ions in the metalloporphyrin ligands. Other metal ions including $Cu^{2+}$, $Mn^{3+}$, $Ni^{2+}$, and $Zn^{2+}$ have also been

checked for the substitution, to easily get the relative analogies. It is interesting that MMPF-5(Co) showed a much more efficient catalytic activity and high selectivity for the epoxidation of *trans*-stilbene, compared with the parent MMPF-5. In addition, Zhou,[116] Yaghi,[117] and Ma's[118] groups simultaneously presented the metalation within the free binding porphyrin-based MOF struts of $\{Zr_6O_4(OH)_4(TCPP-H_2)_3\}_n$ and $\{Zr_6O_8(H_2O)_8(TCPP-H_2)_2\}_n$ ($H_4TCPP-H_2$ = *meso*-tetrakis(4-carboxyphenyl)porphyrin). Both MOFs were reacted with $Fe^{3+}$ or $Cu^{2+}$ salts in solution to yield the related metalated MOFs with a preserved high surface area and chemical stability, respectively. In Zhou and Ma's work, it was also demonstrated that $\{Zr_6O_8(H_2O)_8(Fe-TCPP)_2\}_n$ had a good biomimetic catalytic activity in the oxidation of pyrogallol, 3,3,5,5-tetramethylbenzidine, and *o*-phenylenediamine.

The foregoing examples reveal that in most cases the metal ion substitutions in MOMs are related to the bonding stability of the parent and daughter frameworks. That is, the reaction equilibrium in the substitution finally tends to favor the formation of a more stable phase. Usually, a reversible substitution is always able to occur between the MOFs (such as Zn-MOFs *versus* Co-MOFs, or Zn-MOFs *versus* Ni-MOFs) with similar stability features. Furthermore, we find that most metal ions in the nodes of MOFs can be irreversibly replaced by $Cu^{2+}$ ions, suggesting the high stability of the Cu-based MOMs probably due to the stabilization efficiency from the Jahn–Teller effect of $Cu^{2+}$. In addition, the above-mentioned examples have also demonstrated that either a complete or partial substitution is determined by the preferential coordination of the metal ion, pore size of the MOF, and framework flexibility. On the other hand, the substitution reaction rate tends to vary widely, ranging from a few hours to even one year. The faster substitution rate is often observed at the beginning of the reaction process, because the diffusion of the metal ions always proceeds from the surface to the core in a MOF crystal. Furthermore, the solvent selection also plays a key role in this aspect. For example, methanol is recognized as a more effective solvent than DMF, which can be attributed to the fact that methanol usually forms a relatively small solvation shell around the metal ions in solvent, allowing their faster diffusion and interaction with the framework metal ions. Anyway, all these assumptions are deduced from limited experimental observations; further efforts are required to clarify the substantial mechanisms.

## 2.3.  Coordinated guest molecule substitution

Coordinated guest molecules in the metal ions of MOMs include neutral small molecules and counter ions which usually come from solvents, templates, and metal sources used in their syntheses. These guest molecules play important roles in the formation of MOMs, such as for attaining the required coordination geometry of the central metal ion to sustain the framework structure, or for balancing the charge of the whole molecule. In some cases, the coordination bonds between metal ions and guest molecules are slightly labile so that coordinated guest molecules can be easily substituted or removed without destroying the backbone of the MOMs. A lot of examples can be documented with respect to the removal or

the substitution of coordinated guest molecules in MOFs to modify their properties.[47,53]

For example, Tasiopoulos and co-workers reported the substitution of coordinated DMF molecules by a series of guest solvent molecules of MeOH, EtOH, acetone, THF, and pyridine via a SC–SC transformation in the MOF $[Nd_2(CIP)_2(DMF)_{2.8}(H_2O)_{1.2}]_n$ ($H_3CIP$ = 5-(4-carboxybenzylideneamino)isophthalic acid).[119] Another interesting example was the functionalization of Zr-based MOF $[Zr_6(\mu_3\text{-}OH)_8(OH)_8(TBAPY)_2]_n$ (NU-1000; $H_4TBAPY$ = 1,3,6,8-tetrakis($p$-benzoic acid)pyrene) through the coordinated anion substitution, reported by Hupp and co-workers.[120] NU-1000 possesses an octahedral $Zr_6$ cluster capped by eight $\mu_3$-OH and eight terminal –OH entities. In this work, these terminal –OH groups were substituted by a series of fluoroalkyl carboxylate ligands with different chain lengths when the MOF was reacted with their acids in DMF at 60 °C for 18–24 hours. Finally, these modified MOFs showed enhanced $CO_2$ capture capacities and systematically increased adsorption enthalpies ($Q_{st}$) with the increasing chain length of perfluoroalkanes.[121] Thereafter, the authors in the same group continued their research in this topic by the incorporation of some carboxylate-derived functional entities (isonicotinate, 4-aminobenzoate, and 4-ethynybenzoate) into NU-1000 in a similar procedure. Chemical reactions such as click chemistry, imine condensation, and pyridine quaternization were then used to modify the functionalities of these materials.[122]

An alternative approach in the substitution manipulation of coordinated guest molecules or counter ions in MOMs is to firstly remove these coordinated entities to leave unsaturated metal sites, which are then grafted by other functional molecules. Both generating open metal sites and adding special functional groups can efficaciously modify the pore properties, thereby enhancing for example catalytic activities and gas binding capacities of the resulting MOMs.[123–129] As a typical example, $\{[Cr_3(F,OH)(H_2O)_2O(BDC)_3]\cdot m(H_2BDC)\cdot nH_2O\}_n$ (MIL-101)[52] has been widely explored in this context. The removal of coordinated water molecules in MIL-101 could be achieved through the thermal treatment of the as-synthesized sample under vacuum, to get the dehydrated MIL-101. With this method, Kim and co-workers successfully grafted chiral functional groups into MIL-101 to get $\{[Cr_3O(L_1)_{1.8}(H_2O)_{0.2}F(BDC)_3]\cdot0.15(H_2BDC)\cdot H_2O\}_n$

(CMIL-1) and $\{[Cr_3O(L_2)_{1.75}(H_2O)_{0.25}F(BDC)_3]\cdot0.15(H_2BDC)\cdot H_2O\}_n$ (CMIL-2) by treating the dehydrated MIL-101 with the pre-designed chiral ligands (S)-N-(pyridin-3-yl)-pyrrolidine-2-carboxamide ($L_1$) and (S)-N-(pyridin-4-yl)-pyrrolidine-2-carboxamide ($L_2$), respectively.[130] It was found that these CMIL materials had good catalytic activities in asymmetric aldol reactions between aromatic aldehydes and ketones, with a high enantioselectivity. Similarly, Chang and co-workers demonstrated that ethylenediamine (ED) and diethylenetriamine (DETA) could be grafted into this MOF to give amine-grafted MIL-101, which finally exhibited high catalytic activities in the Knoevenagel condensation reaction.[131]

Using a similar method, Long and co-workers modified a new MOF, $\{Mg_2(DOBPDC)(DEF)_2\}_n$ (DOBPDC = 4,4′-dioxido-3,3′-biphenyldicarboxylate; DEF = N,N′-diethylformamide), to get a functionalized MOF material with excellent $CO_2$ capture ability.[132] As illustrated in Fig. 9, coordinated DEF molecules in this MOF were firstly removed by heating the sample and then N,N′-dimethylethylenediamine (mmen) was grafted to afford $\{Mg_2(DOBPDC)(mmen)_{1.6}(H_2O)_{0.4}\}_n$ (mmen-$Mg_2$(DOBPDC)). As expected, this material displayed an exceptional capacity for $CO_2$ adsorption at low pressures, taking up 2.0 mmol g$^{-1}$ (8.1 wt%) at 0.39 mbar and 25 °C, and 3.14 mmol g$^{-1}$ (12.1 wt%) at 0.15 bar and 40 °C. Interestingly, upon exposure to air the white crystalline powder of $\{Mg_2(DOBPDC)(DEF)_2\}_n$ turned blue and lost crystallinity, implying the collapse of its framework. The mmen-$Mg_2$(DOBPDC) however was stable in air, even staying for 1 week. A very similar study can be found in Long's another report based on an air- and water-stable MOF, $\{H_3[(Cu_4Cl)_3(BTTri)_8(DMF)_{12}]\cdot7DMF\cdot76H_2O\}_n$ (Cu-BTTri-DMF; $H_3$BTTri = 1,3,5-tris(1H-1,2,3-triazol-5-yl)benzene). The desolvated framework of Cu-BTTri, featuring open $Cu^{2+}$ coordination sites, could incorporate ED to afford a functionalized MOF with greatly enhanced affinity and selectivity towards $CO_2$.[133] It should be pointed out that the introduction of alkylamines into the pores of MOFs is a powerful approach to make the materials have a high $CO_2$ adsorption and separation capacity, one of the key factors in the $CO_2$ capture with MOFs. However, the direct preparation of MOFs with alkylamine groups is highly challenging due to the difficulty in the synthesis of related ligands, as well as their MOFs. The substitution strategy discussed here is thus attractive and feasible, with a bright future in this topic.
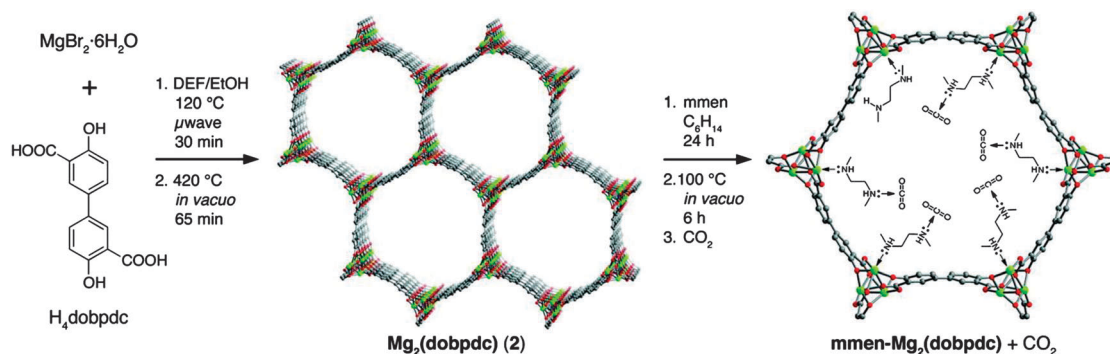


Fig. 9 Stepwise synthesis of amine-appended mmen-$Mg_2$(DOBPDC) MOF, as well as its bonding with $CO_2$ molecules. Reprinted with permission from ref. 132. Copyright 2012 American Chemical Society.
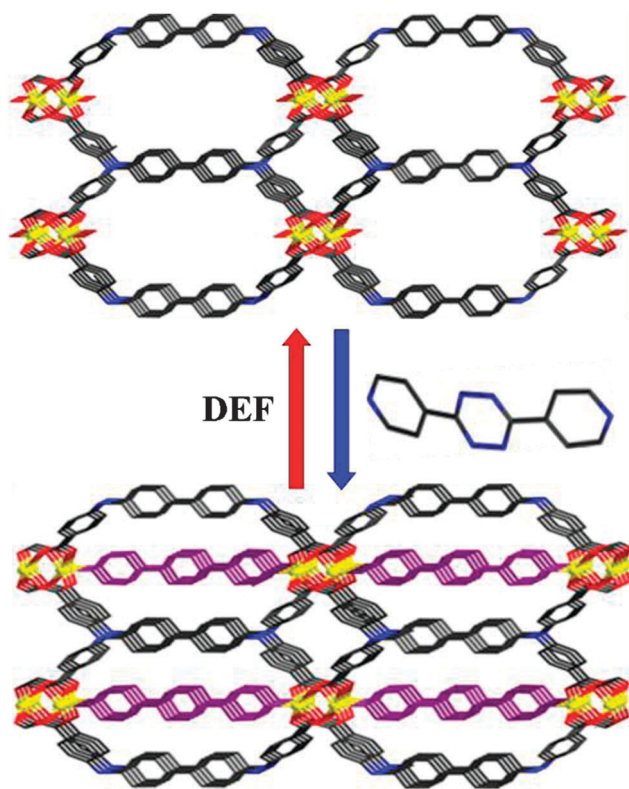
This journal is © The Royal Society of Chemistry 2014

Chem. Soc. Rev., 2014, 43, 5952–5981 | 5961

**Fig. 10** Reversible substitution of coordinated guest molecules by organic linker 3,6-di(4-pyridyl)-1,2,4,5-tetrazine (BPTA) in {[Zn$_2$(TCPBDA)(H$_2$O)$_2$]·30DMF·6H$_2$O}$_n$ to get {[Zn$_2$(TCPBDA)(BPTA)]·23DMF·4H$_2$O}$_n$, and *vice versa*.[134]

Furthermore, as a special example, the substitution of labile solvents by multi-topic organic linkers has been performed to modify the pore size and shape of a MOF, thereby tuning its gas adsorption properties.[134] In this work, Suh and co-workers firstly prepared MOF {[Zn$_2$(TCPBDA)(H$_2$O)$_2$]·30DMF·6H$_2$O}$_n$ (SNU-30; TCPBDA = *N,N,N′,N′*-tetrakis(4-carboxyphenyl)biphenyl-4,4′-diamine). Soaking the yellow crystals of SNU-30 in a DMF solution of 3,6-di(4-pyridyl)-1,2,4,5-tetrazine (BPTA) at 80 °C for 3 hours led to the substitution of each two coordinated water molecule in SNU-30 by a BPTA ligand, resulting in red crystals of {[Zn$_2$(TCPBDA)(BPTA)]·23DMF·4H$_2$O}$_n$ (SNU-31) *via* a SC–SC transformation (Fig. 10). In SNU-31, the original channels in SNU-30 were divided by BPTA linkers. It was demonstrated that the desolvated solid of SNU-30 was able to absorb all N$_2$, O$_2$, H$_2$, CO$_2$, and CH$_4$ gases, whereas desolvated SNU-31 exhibited selective adsorption of CO$_2$ over N$_2$, O$_2$, H$_2$, and CH$_4$. Furthermore, SNU-31 could reversibly liberate BPTA linkers when being immersed in fresh DEF, through the substitution of BPTA ligands by DEF molecules.

In addition, the substitution of the guest solvents or counter ions by multi-topic organic linkers can also lead to the formation of distinct MOFs, in some cases with an enhanced dimension in structures.[46,47] For example, Kitagawa and co-workers reported the transformation of a two-dimensional (2D) layer MOF [Cu(TFBDC)(MeOH)]$_n$ (TFBDC = tetrafluorobenzene-1,4-dicarboxylate) into a 3D MOF [Cu(TFBDC)(DABCO)$_{0.5}$]$_n$ *via* the substitution of coordinated MeOH molecules in the former by a

ditopic organic linker 1,4-diazabicyclo[2.2.2]octane (DABCO).[135] What was more interesting was the demonstration by Chen and co-workers that a 3D pillared-layer MOF {[Zn$_2$(BDC)$_2$(DABCO)]·4DMF·0.5H$_2$O}$_n$ could be firstly transferred into a 2D layer MOF {[Zn$_2$(BDC)$_2$(H$_2$O)$_2$]·DMF}$_n$ in air *via* a SC–SC transformation through the substitution of DABCO ligands by water molecules.[136] And then, this process can be reversed by the substitution of these water molecules in the 2D structure by the DABCO ligands. Similarly, Vittal and co-workers showed that a 2D sheet-like [Cd(μ-BPE)(μ-Br)$_2$]$_n$ (BPE = 4,4′-bipyridylethylene) could be generated through the substitution of coordinated guest molecules and anions in a one-dimensional (1D) chain [Cd(CH$_3$CO$_2$)$_2$(μ-BPE)(H$_2$O)]$_n$[137] by bridging Br$^-$ anions.[138]

Along this line, a new stepwise synthetic approach has been developed for the construction of MOP-based MOFs starting from molecular MOPs acting as reactants.[139–143] This synthesis involves a substitution process of the coordinated guest molecules or anions in MOPs by judiciously selected bridging organic ligands. As the first example in this context, Zhou and co-workers firstly designed and synthesized a soluble and robust MOP [Cu$_2$(CDC)$_2$(DMA)(EtOH)]$_6$ (CDC = 9-*H*-carbazole-3,6-dicarboxylate; DMA = *N,N′*-dimethylacetamide) with an octahedral cage structure, in which all six external Cu$^{2+}$ sites in the vertices of the octahedral cage were occupied by coordinated DMA molecules.[142] As shown in Fig. 11, [Cu$_2$(CDC)$_2$(DMA)(EtOH)]$_6$ underwent a solvent substitution reaction to yield [Cu$_2$(CDC)$_2$(DEF)(EtOH)]$_6$. Further substitution of the coordinated DEF molecules by BIPY was achieved by treating the MOP and BIPY in DEF–EtOH to obtain a 2-fold interpenetrated 3D structural MOF {[Cu$_4$(CDC)$_4$(BIPY)(H$_2$O)$_2$]$_3$}$_n$ with an augmented pcu-a topology. It should be pointed out that MOFs are usually synthesized through a "one-pot" self-assembly approach from all reaction components. The structures of the resulting
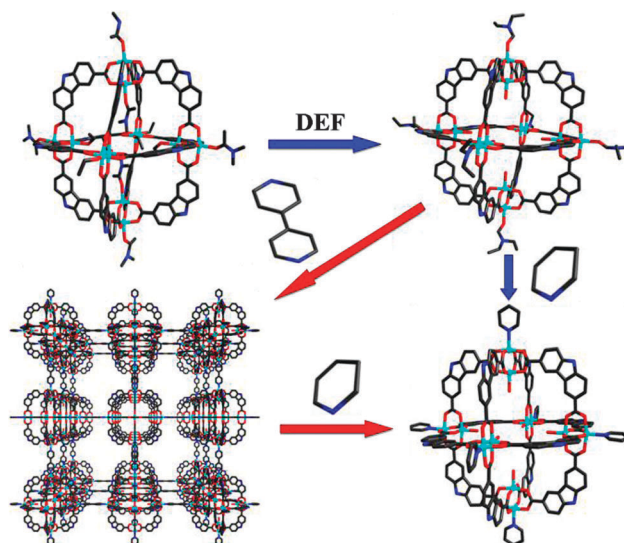


**Fig. 11** The transformation between MOPs [Cu$_2$(CDC)$_2$(S)]$_6$ (S = DMA, DEF, or pyridine) and a MOF {[Cu$_4$(CDC)$_4$(BIPY)(H$_2$O)$_2$]$_3$}$_n$ induced by the substitution reaction between coordinated solvent molecules and bridging ligands.[142]

5962 | *Chem. Soc. Rev.*, 2014, **43**, 5952–5981

This journal is © The Royal Society of Chemistry 2014

products are however unpredictable and difficult to be controlled in some cases, particularly for some MOFs with complicated hierarchical structures, such as the MOP-based MOFs. Clearly, this substitution approach takes a stepwise construction procedure, which can greatly enhance the design and controllability of the resulting MOFs, being widely accessible for the MOF synthesis. Furthermore, in this work based on the substitution of the BIPY by pyridine the MOF was reverted back to the MOP when the former was dissolved in a 4 : 1 DEF/pyridine solvent mixture. This is the first example where a reversible interconversion between MOP and MOF was achieved just through the substitution reaction between coordinated guest molecules and bridging ligands. The pyridine-coordinated MOP could also be obtained through the guest substitution of DEF-coordinated one in solution. Similar substitution of coordinated solvent molecules that led to a stepwise assembly of MOF *via* a MOP intermediate has also been subsequently reported by Su and co-workers,[143] where a 12-connected network $\{[Cu_{24}(5\text{-}NH_2\text{-}mBDC)_{24}(BIPY)_6(H_2O)_{12}]\cdot72DMA\}_n$ with a fcu topology was synthesized using a pre-designed MOP precursor of $Cu_{24}$-$(5\text{-}NH_2\text{-}mBDC)_{24}(DMF)_{12}(H_2O)_{12}\cdot32DMF\cdot6EtOH\cdot12H_2O$.[144]

Besides neutral guest moieties, coordinated anions in some molecular assembles can also be substituted by bridging organic ligands to form MOFs. For example, Wang and co-workers firstly synthesized a pentanuclear tetrahedral compound, $Zn_5(BTZ)_6$-$(NO_3)_4(H_2O)$ (BTZ = benzotriazolate), in which each $Zn^{2+}$ ion in four vertices carried a $NO_3^-$ ion. These coordinated $NO_3^-$ anions were then substituted by several linear carboxylate ligands to extend these molecular clusters to form MOFs (Fig. 12).[145] Experimentally, the reaction of this compound with a series of dicarboxylate ligands of BDC, $NH_2$-BDC, and 4,4′-biphenyldicarboxylate (BPBC) in DMA gave rise to three 3D structural MOFs $\{[Zn_5(BTZ)_6(BDC)_2(H_2O)_2]\cdot7DMA\}_n$, $\{[Zn_5(BTZ)_6(NH_2\text{-}BDC)_2(H_2O)_2]\cdot7DMA\}_n$, and $\{[Zn_5(BTZ)_6$-$(BPDC)_2(H_2O)_2]_{1.5}\cdot10DMA\}_n$, respectively, all having a dia

topological network. Furthermore, Xu and co-workers used similar pentanuclear $Zn_5(BTZ)_6(X)_4(H_2O)$ (X = $NO_3^-$ or $Cl^-$) precursors to synthesize a series of isostructural MOFs also having a dia topology, through the substitution of the coordinated $NO_3^-$ or $Cl^-$ anions by pre-designed tetratopic ligands.[146] Similarly, Zaworotko and co-workers also confirmed a two step assembly of MOFs from a pre-designed trigonal-prismatic molecular compound $[Cr_3(\mu_3\text{-}O)(ISONIC)_6](NO_3)$ (ISONIC = pyridine-4-carboxylate).[147–149]

Apart from using additional reactants, substitution reaction can also occur in a MOF crystal itself. Such a substitution usually leads to the rearrangement and change of the MOF structure, along with bond breakage and regeneration. In most cases, the resulting new compound phases are amorphous, and it is difficult to determine their structures. However, in some examples, after the substitutions the samples remain crystalline, which allows the further analysis of their structures by SXRD or PXRD and the exploration of the associated transformation processes. These coordinated guest substitution induced SC–SC transformations have attracted intense interest in the field of crystal engineering and coordination polymers. Readers interested in these can refer to several excellent reviews for detail.[47,53,54] Herein, we have just listed a few examples to clarify the importance of the substitution reaction in this context.

As a typical example, Rosseinsky and co-workers demonstrated that the MOF $\{[Co_2(BIPY)_3(SO_4)_2(H_2O)_2]\cdot(BIPY)\cdot CH_3OH\}_n$ could undergo a reversible substitution of coordinated water molecules by guest BIPY and methanol molecules in its structure.[150] As shown in Fig. 13, in the structure of this MOF uncoordinated BIPY
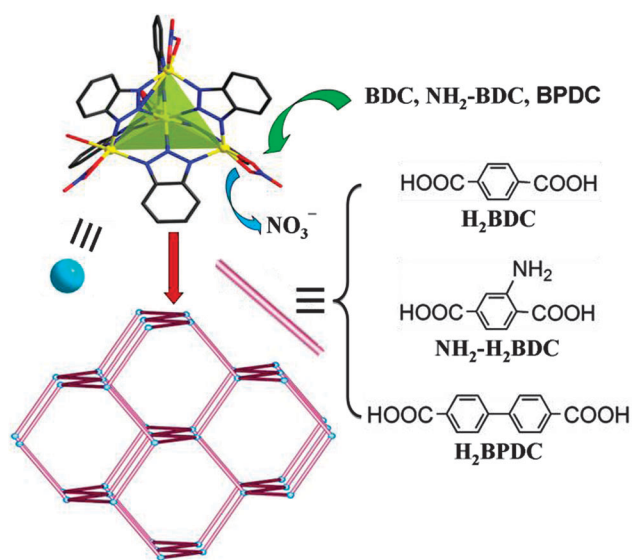


**Fig. 12** Substitution of coordinated $NO_3^-$ anions in $Zn_5(BTZ)_6(NO_3)_4(H_2O)$ by dicarboxylate linkers to form a series of MOFs $\{[Zn_5(BTZ)_6(L)_2(H_2O)_2]\cdot nDMA\}_n$ (L = BDC, $NH_2$–BDC, or BPBC) with a dia net structure.[145]
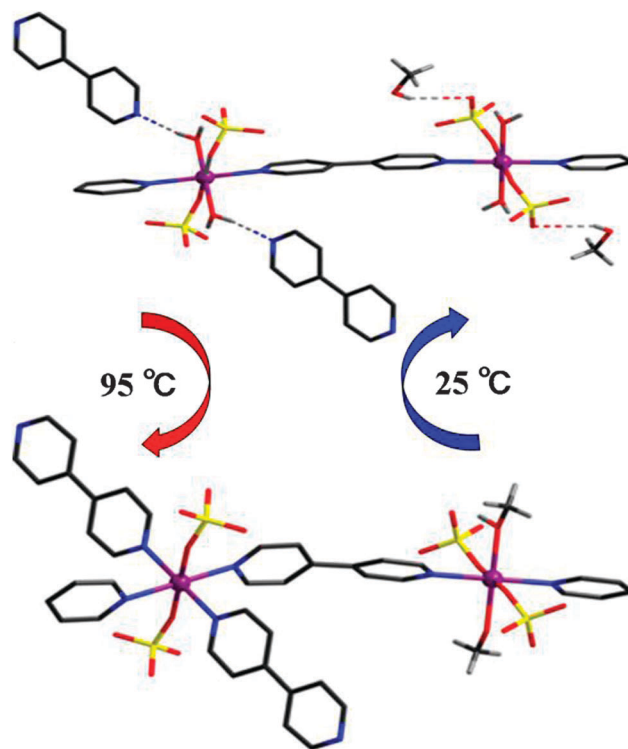


**Fig. 13** Reversible substitution of coordinated water molecules in $\{[Co_2(BIPY)_3(SO_4)_2(H_2O)_2]\cdot(BIPY)\cdot CH_3OH\}_n$ by lattice BIPY and MeOH guest molecules.[150]

This journal is © The Royal Society of Chemistry 2014

*Chem. Soc. Rev.*, 2014, **43**, 5952–5981 | 5963

ligands are H-bonded to the coordinated water molecules, and lattice MeOH molecules are H-bonded to $SO_4^{2-}$ anions. It was found that when pink single crystals of the MOF were heated at 95 °C they gave purple crystals of a new MOF $[Co_2(BIPY)_4(SO_4)_2(CH_3OH)]_n$, where lattice MeOH and BIPY molecules replaced the coordinated water molecules in $\{[Co_2(BIPY)_3(SO_4)_2(H_2O)_2]\cdot(BIPY)\cdot CH_3OH\}_n$. This structural transformation was found to be reversible. In air, atmospheric water could replace the coordinated BIPY and MeOH molecules at room temperature to afford the rehydrated phase. It should be pointed out that this is also an uncommon example, where low-boiling MeOH does not escape from the crystals upon heating but substitutes coordinated water molecules to form a new MOF phase.

In addition, Chen and co-workers also demonstrated an irreversible SC–SC transformation from a 0D structure compound to a 2D MOF based on the guest molecule substitution reaction.[151] They firstly synthesized a discrete compound $Co_2(8\text{-}QOAC)_2(N_3)_2$-$(H_2O)_2$ (8-QOAC = quinoline-8-oxy-acetate) in which each $Co^{2+}$ center was coordinated by one tridentate 8-QOAC, two azido, and one water molecule. When the single crystals of this compound were heated at 150 °C, a new phase of MOF $[Co_2(8\text{-}QOAC)_2(N_3)_2]_n$ was generated. SXRD analysis revealed that the dinuclear unit in the resulting MOF was similar to that in the starting compound. However, each water molecule in the former was substituted by a carboxy O atom from a neighboring dinuclear unit, and thus each dinuclear entity was connected to four neighboring ones by the anti–anti carboxylate bridges to form a 2D layer MOF. This transformation led to a drastic change in the magnetic property from short range coupling to long-range spin-canting antiferromagnetic ordering of the two materials.

As discussed above, a variety of examples of substitutions at metal ions of MOMs were documented. The substitution at metal ions clearly provided a feasible approach to modify or tune not only structures but also associated properties of MOMs, as well as a new strategy to hierarchically synthesize MOFs, for example via MOP intermediates. Particularly, the modifications in properties such as catalysis, magnetism, and gas absorption triggered by the structural transformations can be finally used in designing advanced functional materials for practical applications.

# 3. Substitution at organic ligands

Besides substitution at metal ions, the substitution reaction at organic ligands was also explored and led to plenty of new structures and properties of MOMs, as well as the development of new synthesis strategies for them. Organic ligands used in MOM construction are various and almost countless, and more and more new ligands have been designed and synthesized by virtue of powerful organic synthesis methods for the construction of MOMs.[152–154] Most popularly used ligands are those with carboxylate groups, N-donor groups, or both of them acting as coordination groups. In this section, we discuss the exchange or replacement of organic bridging ligands which directly coordinate to metal ions to sustain the frameworks of MOMs and the chemical modifications of organic ligands in

MOMs without disturbing coordination bonds and framework structures. The former usually leads to new structures and associated properties but the latter mostly modifies the related properties of parent materials.

## 3.1. Organic bridging ligand substitution

Although the structures and pore properties of MOFs or the shapes and sizes of MOPs can be designed in a ''one-pot'' assembly of pre-designed metal-containing nodes and carefully selected organic bridging ligands, and this direct route also appears to be convenient,[11,62,155] it remains difficult to find suitable reaction conditions in some cases. Alternatively, organic ligand substitution,[156–158] also known as solvent-assisted linker exchange (SALE)[50] or postsynthetic ligand exchange (ligand-based PSE),[48] has been approved as a feasible strategy to tune the formation, structures, and properties of MOMs with improved functions. This method indeed has been widely used in discrete coordination complexes[159] or organo-metallic species.[160–164] Like the substitution at metal ions, all three kinds of two-phase substitutions of solid–solid, solid–liquid, and liquid–liquid (only for soluble MOPs) have also been observed in the organic bridging ligand substitution of MOMs. Furthermore, in some cases, partial substitution occurred and allowed to access mixed-ligand species, which are however difficult to achieve by means of a direct synthetic approach.

For example, Choe and co-workers observed a series of SC–SC transformations of MOFs induced by the organic bridging ligand substitutions (Fig. 14).[165] They firstly synthesized two parent MOFs $[Zn_2(ZnTCPP)(DPNI)]_n$ (PPF-18) and $[Zn_2(ZnTCPP)(DPNI)_{1.5}]_n$ (PPF-20) (DPNI = $N,N'$-di-4-pyridylnaphthalenetetracarboxydiimide). The former has a 2D bilayer structure of porphyrin paddle-wheel layers, whereas the latter has a 3D pillared-layer framework, and in both the 2D porphyrin paddle-wheel layers are coordinately



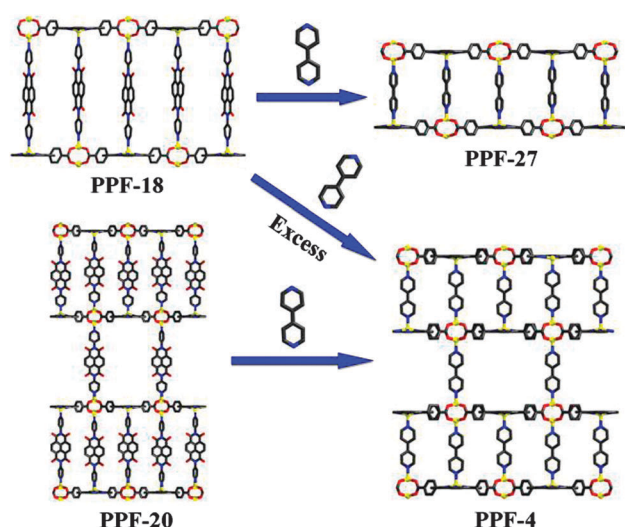**Fig. 14** Schematic representation of bridging organic ligand substitutions in MOFs $[Zn_2(ZnTCPP)(DPNI)]_n$ (PPF-18) and $[Zn_2(ZnTCPP)(DPNI)_{1.5}]_n$ (PPF-20) to form $[Zn_2(ZnTCPP)(BIPY)]_n$ (PPF-27) and $[Zn_2(ZnTCPP)(BIPY)_{1.5}]$ (PPF-4).[165]

**5964** | *Chem. Soc. Rev.*, 2014, **43**, 5952–5981

This journal is © The Royal Society of Chemistry 2014

connected by DPNI ligands on the axial $Zn^{2+}$ sites of the paddle-wheel entities.[166] When the crystals of PPF-18 were immersed in a DEF–EtOH solution of BIPY, the DPNI ligands were replaced by the BIPY, resulting in another 2D layer MOF [$Zn_2$(ZnTCPP)-(BIPY)]$_n$ (PPF-27). PPF-27 was confirmed to be inaccessible as a single phase *via* a one-step synthesis approach. When excess BIPY (>2 equiv.) was used, additional BIPY linkers coordinated to the paddle-wheel $Zn^{2+}$ sites between the bilayers, resulting in a 3D MOF [$Zn_2$(ZnTCPP)(BIPY)$_{1.5}$] (PPF-4).[167,168] A similar situation was also observed in PPF-20, and a substitution procedure in the case of PPF-18 gave the single phase material of PPF-4. Another example of organic bridging ligand substitution in a 3D pillared-layer structure was reported by Hupp and co-workers based on the MOF {$Zn_2$($H_2$-TCPP)($M^2$-L)}$_n$ (ZnM²-RPM; L = 5,15-dipyridyl-10,20-bis(pentafluorophenyl)porphyrin),[169] where dipyridyl-porphyrin-Zn($\text{II}$) (Zn-DIPY) struts could be replaced by $M^2$-DIPY ($M^2$ = $2H^+$, $Al^{3+}$, and $Sn^{4+}$).[170] Subsequent catalysis experiments based on the ring-opening of styrene epoxide through reaction with trimethylsilylazide (a reaction known to be catalyzed by Lewis acid) indicated that Zn2H- and ZnSn-RPM did not have a catalytic activity, whereas ZnAl-RPM showed significant catalytic capacity due to its comparatively strong Lewis acidity.

Apart from the neutral organic bridging ligands, negatively charged carboxylate ligands can also be substituted in some MOFs. Rosi and co-workers reported the synthesis of three isoreticular analogues of {[$Me_2NH_2$]$_4$[$Zn_8$(AD)$_4$(BPDC)$_6$O$_2$]·49DMF·31$H_2$O}$_n$ (Bio-MOF-100; AD = adenine[171]), Bio-MOF-101, -102, and -103, by using a stepwise dicarboxylic ligand substitution procedure, where shorter ligands were replaced by

longer ones *via* a SC–SC transformation (Fig. 15).[172] Bio-MOF-100 has a 3D structure composed of [$Zn_8$(AD)$_4$O$_2$]$^{8+}$ clusters periodically linked by BPDC ligands. It was found that Bio-MOF-101 with 2,6-naphthalenedicarboxylate (NDC) linkers could be obtained *via* a direct synthesis procedure; however, the analogues with organic linkers longer than BPDC could not be obtained at this stage. The organic bridging ligand substitution was thus used herein for accessing more porous analogues of bio-MOF-100 with longer linkers. The conversion between bio-MOF-101 and bio-MOF-100 was achieved by soaking bio-MOF-101 in a BPDC–DMF–NMP solution (NMP = *N*-methylpyrrolidinone). The resulting crystals were transparent and slightly cracked. $^1$H NMR spectra revealed that only adenine and BPDC linkers without NDC existed in the product, indicating a complete substitution of ligand NDC by BPDC. Similarly, bio-MOF-102 could be obtained by using the same procedure of substituting BPDC in bio-MOF-100 with the longer azobenzene-4,4′-dicarboxylate (ABDC) ligand. And, soaking the crystals of Bio-MOF-102 in the much longer 2′-amino-1,1′:4,1″-terphenyl-4,4″-dicarboxylate ($NH_2$-TPDC) ligand solution yielded light orange crystals of bio-MOF-103, even if complete substitution was not achieved in this transformation. Interestingly, the volume changes of the crystals in these stepwise ligand substitutions have also been directly observed.

On the other hand, a partial organic ligand substitution can lead to the immobilization of functional molecules on the surface of a regular MOF crystal. Kitagawa and co-workers performed such a study based on two MOFs, [$Zn_2$(BDC)$_2$(DABCO)]$_n$ (**F1**) and [$Zn_2$(NDC)$_2$(DABCO)]$_n$ (**F2**),[173] where their crystal surfaces were functionalized by the fluorescent dye molecule of mono-carboxylic boron dipyrromethene (BODIPY).[174] Immersing single crystals of **F1** or **F2** in a dehydrated DMF solution of BODIPY dye resulted in their coloration due to the substitution of dicarboxylate ligands BDC and NDC by BODIPY on the crystal surface. As illustrated in Fig. 16, in **F1** and **F2**, only four faces of the rectangular prismatic crystals exposed carboxylate entities, and therefore only these faces showed coloration during the substitution process. They also explored the coloration of [$Cu_3$(BTC)$_2$($H_2$O)$_3$]$_n$ (HKUST-1) crystals by a similar procedure.[175] HKUST-1 crystals are octahedral with all faces exposing carboxylate sites. As expected, all the faces were covered by a monolayer of the fluorescent dye after the substitution reaction. These surface-modified MOF crystals were then detected by using confocal laser scanning microscopy (CLSM) to present attractive images as shown in Fig. 16. These results demonstrated a stepwise method of using the regular structure to facilitate the immobilization of functional molecules onto MOF particles.

As observed in metal center substitution, organic ligand substitution can also take place in some comparatively stable/robust MOFs, such as ZIFs, UiO, and MIL series. Hupp and co-workers reported the first example of solvent-assisted linker exchange (SALE) in ZIFs.[50] A cadmium-based ZIF, [Cd(EIM)$_2$]$_n$ (CdIF-4; EIM = 2-ethylimidazolate[176]), was chosen as the parent framework, which has a rho topology and large apertures. To perform the organic ligand exchange, CdIF-4 crystals were immersed in a DMF solution of 2-nitroimidazole (HNIM) at 100 °C. After 48 hours, it was found that all of EIM ligands in
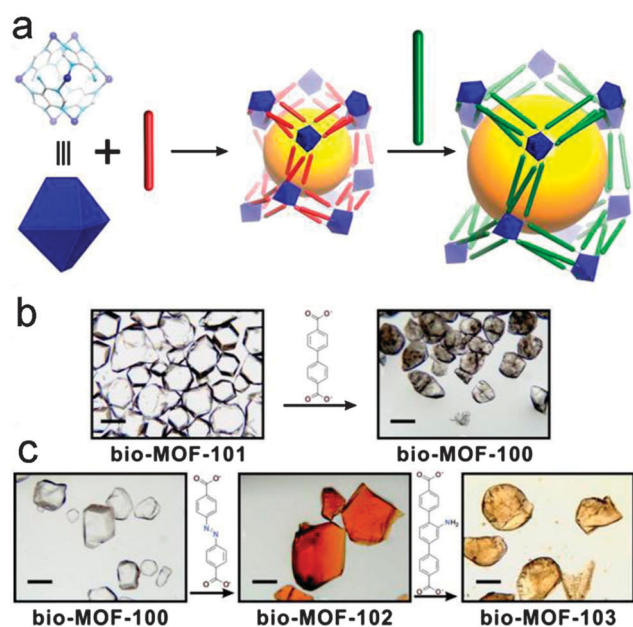


**Fig. 15** (a) Scheme representing the pore expansion strategy. (b) Bio-MOF-101 was converted to bio-MOF-100 *via* the ligand exchange of BPDC. (c) BPDC in bio-MOF-100 was substituted by ABDC to yield bio-MOF-102; thereafter ABDC in bio-MOF-102 was substituted by $NH_2$-TPDC to yield bio-MOF-103. Reprinted with permission from ref. 172. Copyright 2013 American Chemical Society.

This journal is © The Royal Society of Chemistry 2014

*Chem. Soc. Rev.*, 2014, **43**, 5952–5981 | **5965**

Fig. 16 (a) Schematic representation of ligand substitution on the crystal surface. (b) and (c) Representations of surface-modified crystals (left), CLSM images (middle) and transmission images (right) of BODIPY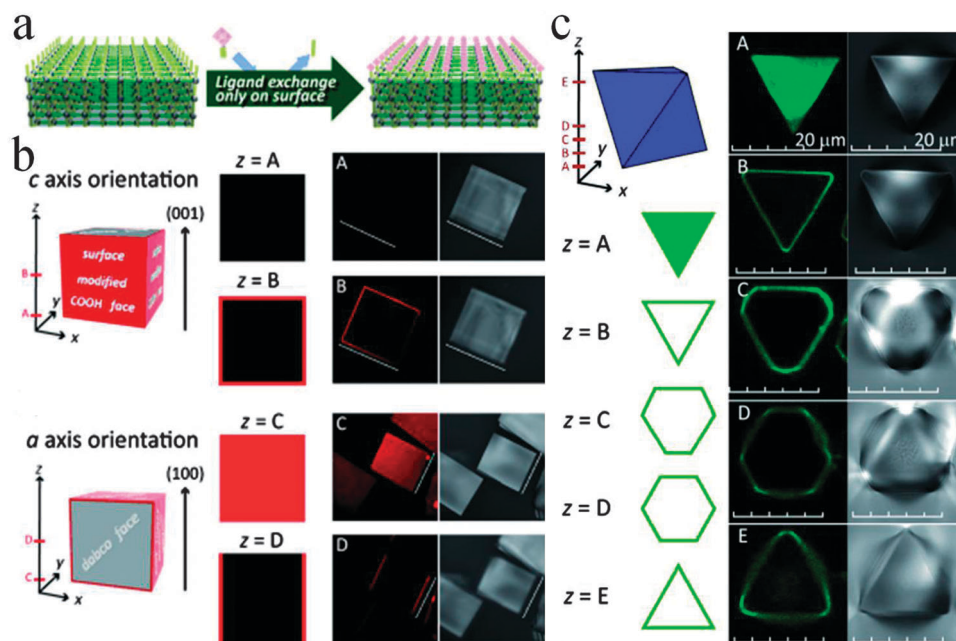 functionalized **F2** and HKUST-1 crystals, respectively. Reprinted with permission from ref. 174. Copyright 2010 WILEY-VCH Verlag GmbH & Co. KGaA, Weinheim.

CdIF-4 were replaced by NIM ligands to give $[Cd(NIM)_2]_n$ (CdIF-9[176]), and the crystals maintained their original shapes. PXRD also confirmed the integrity of the original rho framework. The resulting CdIF-9 possessed one of the highest surface areas among the reported ZIFs. A similar complete substitution was also achieved when using 2-methylimidazole (HMIM) to substitute EIM under similar conditions, giving $[Cd(MIM)_2]_n$ (SALEM-1) again with a preserved rho topological structure. Further studies revealed that the exposure of SALEM-1 to a DMF solution of excess HEIM or HNIM could also lead to the formation of CdIF-4 and CdIF-9, respectively. However, the reversible conversions from CdIF-9 to CdIF-4 and SALEM-1 were inaccessible under similar conditions. Another example of organic bridging ligand substitution in ZIFs was subsequently reported by Cohen and co-workers.[49] They examined the ligand exchange in dichloro-substituted Zn$^{2+}$-based ZIF-71[102] by exposing its crystals to a MeOH solution of 4-bromo-1*H*-imidazole at 55 °C for 5 days. It was found that in the process, 30% of the ZIF-71 was transformed after the substitution reaction.

Cohen and co-workers also explored the organic ligand substitution in the UiO-66 and MIL series.[48,51] In the UiO-66 system it was found that the substitution reaction could take place through a reaction between two MOFs, with both in the solid state (a solid–solid process) (Fig. 17). In this work, UiO-66-NH$_2$ and UiO-66-Br were firstly synthesized by using the ligands 2-amino-1,4-benzenedicarboxylate (NH$_2$-BDC) and 2-bromo-1,4-benzenedicarboxylate (Br-BDC), respectively.[177] Then, a mixture of UiO-66-NH$_2$ and UiO-66-Br particles was suspended in water for 5 days at room temperature. ATOFMS analysis of the resulting sample indicated that more than 50% of the UiO-66-X particles underwent a ligand exchange. At an elevated reaction
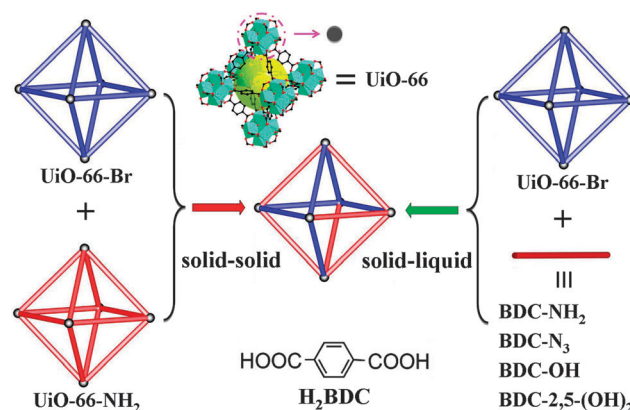


Fig. 17 Schematic representation of solid–solid or solid–liquid ligand substitutions in the UiO-66 series.[177]

temperature of 85 °C it was confirmed that nearly all of the particles underwent ligand exchange. It was also found that the ligand exchange rate in this system strongly correlated with the solvents used, with water achieving the highest rate followed by DMF, methanol, and chloroform. In addition, a solid–liquid ligand exchange was also explored in this system. UiO-66-Br was suspended in an aqueous solution of NH$_2$-BDC for 5 days to get UiO-66-NH$_2$(Br), where the ligand exchange rates were found to be temperature dependent. For example, at room temperature about 9% of Br-BDC was replaced by NH$_2$-BDC, but at 85 °C, the substitution rate was about 76%. Following the same procedure, it was also confirmed that 2-azido-1,4-benzenedicarboxylate (N$_3$-BDC), 2-hydroxy-1,4-benzenedicarboxylate (OH-BDC), and 2,5-dihydroxy-1,4-benzenedicarboxylate (2,5-(OH)$_2$-BDC)

5966 | *Chem. Soc. Rev.*, 2014, 43, 5952–5981

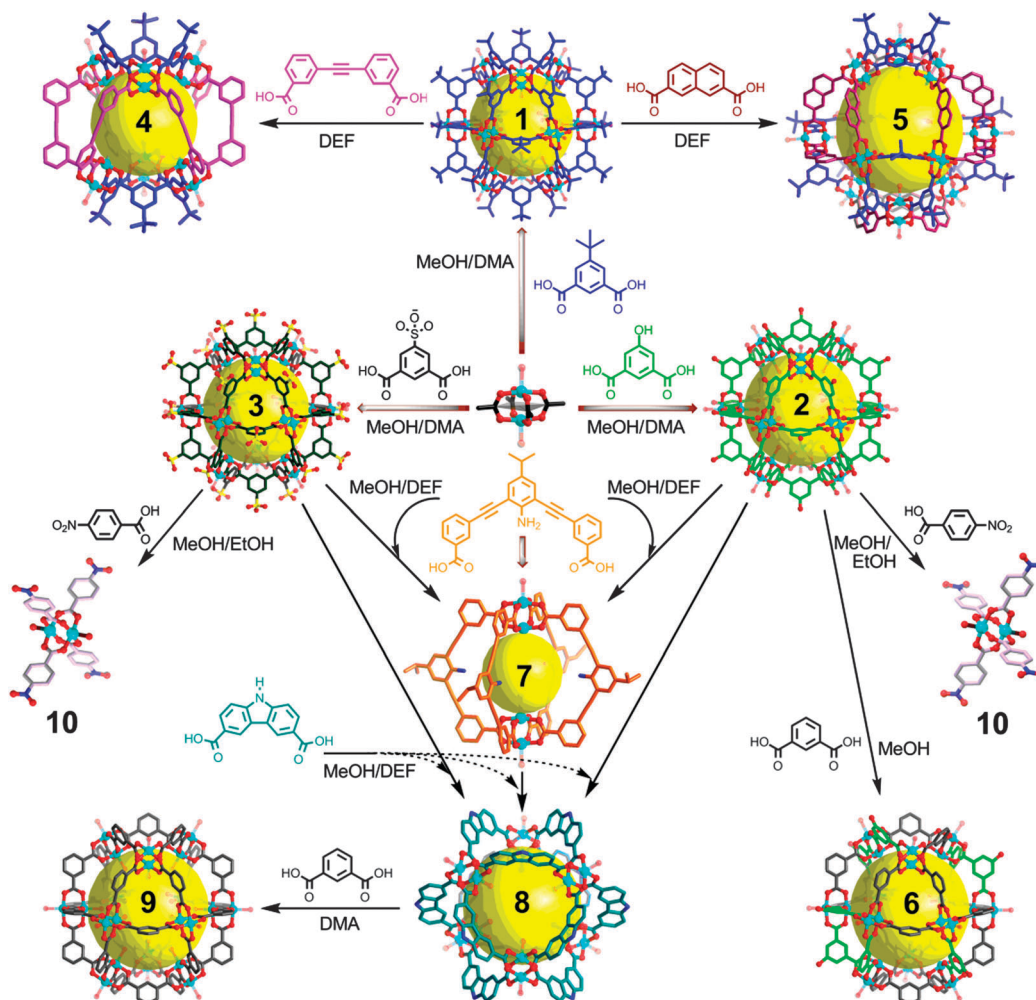This journal is © The Royal Society of Chemistry 2014

Fig. 18 Schematic representation of the synthesis of MOPs 1–3 and their transformation to MOPs 4–9 and compound 10, all based on the ligand substitution reaction. Reprinted with permission from ref. 182. Copyright 2010 Nature Publishing Group.

could partially substitute BDC in UiO-66 under similar conditions, with the retention of the crystalline samples in all cases.

Similarly, the same group also studied the solid–solid substitution reaction in the MIL series. To do this for MIL-53(Al)-NH$_2$[178] and MIL-53(Al)-Br,[98] the two MOFs were mixed together and suspended in water at 85 °C for 5 days. ATOFMS analysis showed that approximately 56% of the resulting materials contained both ligands, implying that ligand exchange occurred between more than half of each MOF particle. For the MIL-68(In) system, two types of solids of MIL-68(In)-NH$_2$ and MIL-68(In)-Br[92] were mixed together and incubated in DMF at 55 °C for 5 days to get about 42% of particles that contained both Br- and NH$_2$-containing ligands. However, attempts to examine MIL-101(Cr)[52] with respect to the ligand substitution failed, probably due to the high kinetic inertness of the Cr$^{3+}$ ions in the MOF. The foregoing results demonstrated that despite structural robustness, ligand substitutions could still be readily carried out on some stable and inert MOFs through a solid–solid or a solid–solution substitution reaction process.

Besides that achieved in MOFs, ligand substitution can also take place in MOPs to get new members, which sometimes are

difficult to access by a direct reaction of metal ions and organic ligands.[179–183] Zhou and co-workers for the first time extended the ligand substitution into the interconversion between MOPs. An "organic-bridging-ligand-substitution" synthetic strategy was developed to prepare and isolate a series of novel MOPs with various compositions, pore sizes and shapes, and functionalities.[182] As shown in Fig. 18, three soluble MOPs [Cu$_{24}$(5-$t$-Bu-1,3-BDC)$_{24}$(S)$_{24}$] (1), [Cu$_{24}$(5-OH-1,3-BDC)$_{24}$(S)$_{24}$] (2), and Na$_6$H$_{18}$[Cu$_{24}$(5-SO$_3$-1,3-BDC)$_{24}$(S)$_{24}$] (3) were firstly prepared by the substitution reaction between Cu$_2$(OAc)$_4$·2H$_2$O and three dicarboxylic ligands. Reaction of these soluble MOPs with several new ligands in solution gave other MOPs of 6–9. Particularly, MOPs 4 and 5 with mixed ligands have been obtained through a partial ligand substitution in this system, which were quite difficult to achieve through a direct self-assembly reaction between the two types of ligands and the metal ions. Finally, a monocarboxylic ligand terminated the formation of MOPs again based on the ligand substitution reaction to give a simple dinuclear compound 10. This work has opened up a new way for accessing novel MOPs through the bridging ligand substitution reaction. In principle, by judiciously
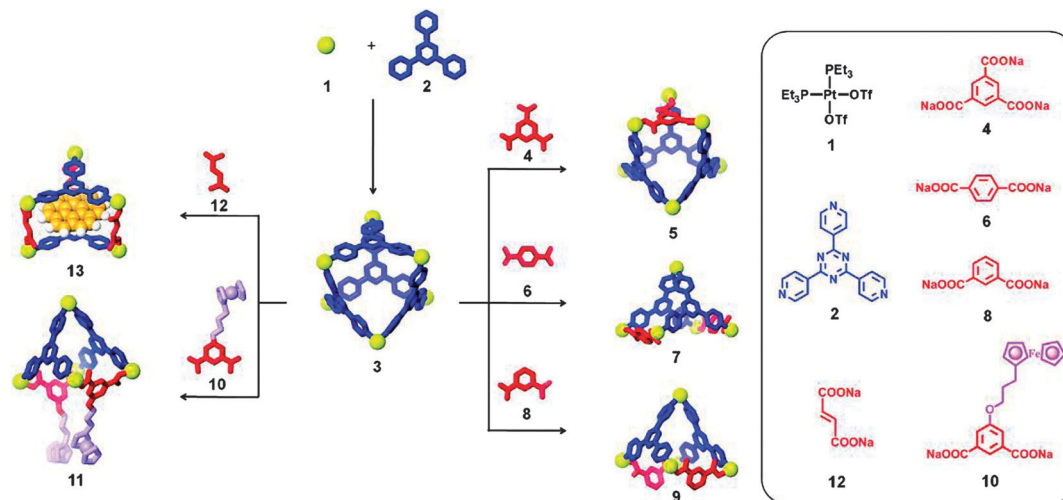
This journal is © The Royal Society of Chemistry 2014

Chem. Soc. Rev., 2014, 43, 5952–5981 | 5967

**Fig. 19** Schematic representation of component substitution, structural modifications, and functional evolution induced by the ligand substitution in a MOP (**3**). Reprinted with permission from ref. 183. Copyright 2011 American Chemical Society.

selecting a suitable solvent system, this method can be applied in the preparation of many novel MOPs and even MOFs as discussed above. This general approach is also useful in constructing and isolating other complex metal–organic supramolecular architectures.

A similar example of bridging ligand substitution in MOPs was also reported by Stang and co-workers.[183] In their work, the observed structural transformation achieved by the substitution can be divided into two situations: a ligand in the initial MOP is replaced by another ligand with a similar linkage mode and the same number of binding sites to give rise to a new MOP with the same shape but different composition; and the incorporation of a new ligand with different shape and numbers of binding sites leads to a drastic change in the size and shape of the resulting new MOPs. As shown in Fig. 19, these transformations started from a two-component [6+4] MOP (**3**). Experimentally, an acetone solution of **3** was added into an aqueous solution of tricarboxylate ligand **4**, giving the modified three-component MOP **5**, which is structurally similar to **3**. By using several bicarboxylate ligands (**6**, **8**, **10**, and **12**) to react with **3** again in water–acetone one could obtain MOPs **7**, **9**, **11**, and **13** with different shapes. Organic bridging ligand substitution in these MOPs thus resulted in a series of new members with not only different compositions but also distinct sizes and geometric shapes, being also quite interesting for supramolecular self-assembly of complex systems.

It should be pointed out that the substitutions taking place at metal ions or organic bridging ligands in MOFs and MOPs can be essentially attributed to the reversible nature of the coordination bonds between metal ions and organic ligands in these materials. In this way, a mechanism can be speculated: when such a substitution reaction takes place, the cleavage of partial chemical bonds in the original framework produces an intermediate state with lattice defects to encounter foreign components to finally transform into a more stable substituted state, which promotes the accomplishment of the reaction process. This process also allows access to novel products (mixed metal ions or mixed organic ligands in one lattice) that

may be thermodynamically unfavorable in the transformation process, as discussed above.

## 3.2.  Chemical modification in organic ligands

Another powerful and versatile method to chemically modify the properties of MOMs consists of adding functional groups on organic ligands, without destroying the original framework skeleton.[177,178,184–186] Chemical modification initially recognized by Robson[187] and recently carried forward by Cohen and others has been widely used in functionalizing MOFs by the rational introduction of new entities into parent structures, mainly manipulated on organic ligands.[56,188] Several excellent reviews/book chapters on the topic of post-modification (synthesis) of MOFs cover most of the work in this aspect;[56–59,188,189] here we only list some selective examples to emphasize the substitution reactions that take place in organic ligands (covalent modification), as well as the loading of metal ions onto open organic coordination sites (coordination modification) to functionalize MOMs.

Among the examples of chemical covalent modification of MOMs, amine-tagged MOFs such as those with the NH₂-BDC ligand have been extensively explored in this context. Several such MOFs have been used as platforms to graft various functional groups such as aldehydes, isocyanates, anhydrides, and sulfonates.[190–192] For example, Yaghi and co-workers showed that the ring-opening covalent modifications in $[Zn_4O(NH_2\text{-}BDC)_3]_n$ (IRMOF-3)[184] with 1,3-propane sultone or 2-methylaziridine could give functional products without destroying the crystallinity and porosity of the original MOF.[193] In the case of using 1,3-propane sultone, the resulting MOF encapsulated free sulfonate groups within its pores, while the modification with 2-methylaziridine produced free alkylamine groups in the pores. The introduction of these functional groups thus greatly changed the pore properties of the resulting MOFs. Similar ring-opening covalent modifications have also been achieved with cyclic anhydrides acting as graft reagents in Cohen and co-workers' work.[194,195] Alternately, click chemistry
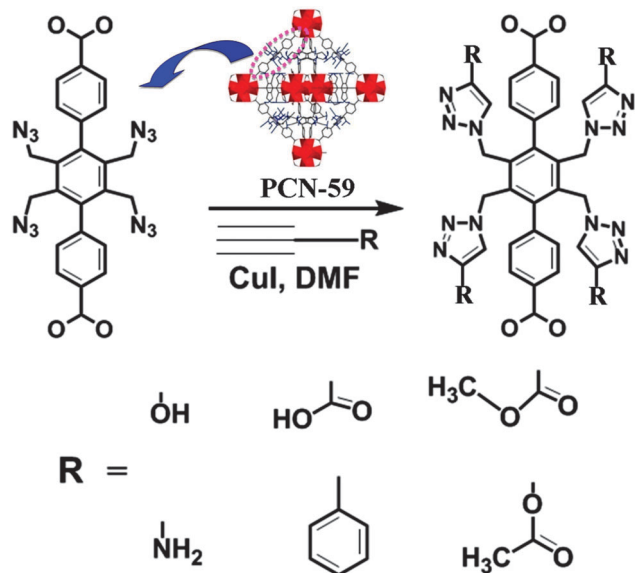
**Fig. 20** Schematic representation of grafting various functional groups onto the pore walls of $\{Zr_3O_2(OH)_2(TPDCR)_3\}_n$ [R = $4CH_2N_3$ (PCN-59)] via the click reactions on ligands.[201]

typically referring to the 1,3-dipolar cycloaddition between an azide and an alkyne[196] has also been used in the covalent ligand modification of MOFs.[197–199] The first example was reported by Sada and co-workers on the MOF $[Zn_4O(N_3)_3]_n$ (N3-MOF-16; $H_2N_3$ = $2',5'$-bis(azidomethyl)-[1,1':4',1''-terphenyl]-4,4''-dicarboxylic acid).[200] The click reactions of the azide groups in the MOF with various alkynes were successfully performed, without leading to any decomposition of the original MOF network. Similarly, Zhou and co-workers also reported the click modifications of pore properties in $Zr^{4+}$-based MOFs with azide functionalized terphenyl-4,4''-dicarboxylate (TPDCR) ligands.[201] In this work, two MOFs, $\{Zr_3O_2(OH)_2(TPDCR)_3\}_n$ (PCN-58, R = $2CH_2N_3$; PCN-59, R = $4CH_2N_3$), were firstly synthesized and used to be clicked by various alkynes with different functional groups (Fig. 20). After the click modifications, the resulting materials showed similar PXRD patterns to those of PCN-58 and PCN-59, respectively, indicating the retention of the framework structures. With these modifications various functional groups were thus grafted into the MOF pores, which led to tuned $CO_2$ selective adsorption ability over $N_2$ of these modified materials.

Besides covalent modification, the coordination modification of ligands in MOFs was also explored. For example, Lin and co-workers reported such a study in homochiral MOF $\{[Cd_3Cl_6L_3]\cdot 4DMF\cdot6MeOH\cdot3H_2O\}_n$ constructed from a bipyridine ligand, $(R)$-6,6'-dichloro-2,2'-dihydroxy-1,1'-binaphthyl-4,4'-bipyridine (L), containing additional orthogonal chiral 2,2'-dihydroxy coordination groups.[202] Treatment of this MOF with $Ti(O^iPr)_4$ gave the modified MOF material, in which $Ti(O^iPr)_2$ entities were coordinated to the binaphthol sites of the L ligand. This material was then used as a catalyst in the addition of $ZnEt_2$ to aromatic aldehydes, to afford chiral secondary alcohols at up to 93% enantiomeric excess (ee). It was also found that only one-third of the binaphthol sites in ligands were modified with $Ti(O^iPr)_4$, typically a partial coordination modification. Subsequent efforts by the same group produced a series of chiral MOFs with functionalized pores, realized again by using a similar coordination modification of ligands.[203] These modified MOFs also showed high activities in the asymmetric catalysis of the above-mentioned reactions. It was also demonstrated that the enantioselectivities of these reactions could be varied by tuning the pore sizes of these MOFs, by adding different functional entities.

Another typical example of ligand coordination modification in MOFs was reported by Long and co-workers.[204] In this study, a MOF $[Al(OH)(BYPDC)]_n$ (MOF-253) was constructed through the coordination of Al(OH) chains with the carboxylate groups of the ligand 2,2'-bipyridine-5,5'-dicarboxylate (BYPDC), leaving free chelating sites of 2,2'-bipyridine suitable for the metal coordination modification. The 2,2'-bipyridine sites in MOF-253 were then coordinated by $Cu^{2+}$ or $Pd^{2+}$ ions, experimentally by soaking MOF-253 in an acetonitrile solution of $Cu(BF_4)_2$ or $PdCl_2$, to obtain the functionalized materials (Fig. 21). It was found that in both cases, more than 90% and 80% of the BYPDC ligands were metalated by $Cu^{2+}$ and $Pd^{2+}$ ions, respectively. Significantly, an enhanced selectivity in binding $CO_2$ over $N_2$ under typical flue gas conditions was observed in the Cu-modified MOF-253. This material is thus potentially useful in carbon capture. It could also be speculated that the $Pd^{2+}$-modified MOF should be a good candidate for application in catalysis, but related reports are not documented up to date.

Clearly, the chemical modification in organic ligands has been a growing hot topic in the functionalization of MOFs. Numerous chemical reactions have been explored in this aspect, generally included in the covalent modification.
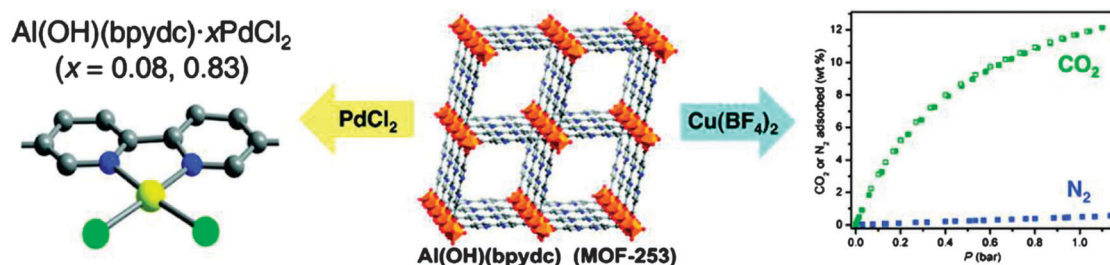


**Fig. 21** Schematic representation of coordination modification in $[Al(OH)(BYPDC)]_n$ (MOF-253) with $PdCl_2$ (left). An enhanced selectivity for binding $CO_2$ over $N_2$ observed in the Cu-modified MOF-253 (right). Reprinted with permission from ref. 204. Copyright 2010 American Chemical Society.

The resulting new functional materials are usually difficult to be synthesized by a direct reaction between related functionalized ligands and metal ions. This is because a slight modification in the ligand could lead to the formation of distinct MOFs even if the reaction is carried out under similar synthesis conditions. To achieve these modifications, a careful selection of reaction type, reactant, and reaction condition is thus quite important. Overall, chemical modification in organic ligands has indeed paved the way for the production of novel MOFs with unprecedented structural complexity and a broad range of properties and functions.

# 4. Substitution at free guest molecules

As porous materials, the study of host–guest chemistry in them is one of the most promising applications of MOFs and MOPs.[205–209] Free guest molecules in the cavities of such materials are not so free, but usually involved in several types of interactions such as H-bonding, $\pi \cdots \pi$ stacking, or weak interactions with metal sites or ligands. Host–guest chemistry including guest inclusions, exchanges, and separations induced by the substitution of guest molecules has indeed been investigated in MOFs and MOPs. In this regard, these materials are potentially useful, such as in molecular sensing, inclusion and recognition, separation, and they even act as molecular reactors for specific reactions performed inside their pores. Particularly, in some cases the guest substitution takes place in a material that still remains crystalline, and thus the exact nature of interactions between the host and the guest can be studied in detail by SXRD to give important information. Guest molecules in MOFs and MOPs can be neutral, cationic, and anionic, which are separately discussed with respect to their associated substitutions in the following sections. It should be pointed out that a large number of examples treating the host–guest chemistry in MOPs or supramolecular cages have been reported, and summarized in several reviews.[210–214] A discussion of only those related to MOFs and functional modifications triggered by guest substitutions is given here.

## 4.1. Neutral guest molecule substitution

Neutral solvent molecule exchange or substitution is commonly found in MOFs and MOPs research; hence we do not give a detailed discussion here. For example, in activating a MOF as-synthesized in high-boiling point solvents (such as DMF, DMA, DEF, or DMSO), usually these solvent molecules are firstly exchanged by low-boiling point ones, so that the sample can be desolvated at a lower temperature to avoid the collapse of the framework at high temperature. Apart from small solvent guests, large organic molecules can also be introduced into the pores of MOFs or MOPs *via* the guest substitution, to perform the interesting phenomena of host–guest chemistry or endow them with unique properties of the host frameworks and/or the guest molecules.

For example, Fujita and co-workers reported the guest molecule substitution in a 3D MOF $\{[(ZnI_2)_3(TPT)_2]\cdot5.5(nitro-benzene)\}_n$ (TPT = 2,4,6-tris(4-pyridyl)triazine).[215] It was found
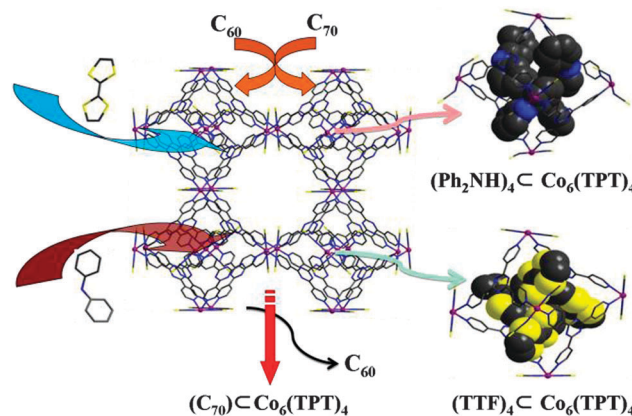


Fig. 22 Schematic representation of the guest molecule encapsulations and separations in $\{[(Co(SCN)_2)_3(TPT)_4]_n\cdot x(G)\}_n$ based on the guest substitutions.[217]

that the nitrobenzene molecules in the MOF pores can be substituted by some large organic molecules including triphenylene, anthracene, and perylene. SXRD analysis revealed an efficient stacking between the included planar guest molecules and the ligands of the MOF skeleton. The crystals of the inclusion complexes also presented a drastic color change because of the strong donor–acceptor interactions between the electron-deficient ligand and electron-rich guests.[216] Another example reported by the same group is the guest substitution in a MOF $\{[(Co(SCN)_2)_3(TPT)_4]_n\cdot x(G)\}_n$ (G = guest molecules) with $Co_6(TPT)_4$ MOP cages acting as molecular building units (Fig. 22).[217] Treatment with a saturated toluene solution of tetrathiafulvalene (TTF) resulted in the color change of the MOF crystals from orange to black. SXRD analysis revealed that four TTF molecules were encapsulated in each $Co_6(TPT)_4$ cage chamber in the MOF framework. Similarly, the $(TTF)_4\cdot Pd_6(TPT)_4$ could also be obtained by suspending excess TTF in an aqueous solution of discrete $Pd_6(TPT)_4$ MOP cage[218] based on again the guest exchange. Further studies demonstrated that both the MOF and the MOP could also reversibly upload and release diphenyl-amine ($Ph_2NH$), $C_{60}$, and $C_{70}$ molecules in toluene. It was found that this MOF was able to take about 35 wt% $C_{60}$ and 34 wt% $C_{70}$ in their saturated toluene solutions, respectively. Interestingly, when the crystals of the MOF were immersed in a fullerene mixture, $C_{70}$ was preferentially absorbed over $C_{60}$. On the basis of these results, the Fujita group developed a general method for the crystallographic structural analysis of non-crystalline guests on a nanogram to microgram scale by loading them into the pores of a crystalline and structurally well-determined MOF host framework.[219]

In the guest substitution, some MOFs showed a selective uptake of incoming guests as mentioned above, which is highly desirable for their application in the separation or purification of a molecular mixture. As another example, Dong and co-workers reported a 3D MOF $\{[Cd(ClO_4)_2(L)_2]\cdot2CH_2Cl_2\}_n$ (L = 4-amino-3,5-bis(4-pyridyl-3-phenyl)-1,2,4-triazole), which showed a selective uptake ability towards different small organic molecules.[220,221] It was found that when exposed to air, the desolvated MOF $[Cd(ClO_4)_2(L)_2]_n$ (removing $CH_2Cl_2$) converted into a hydrated

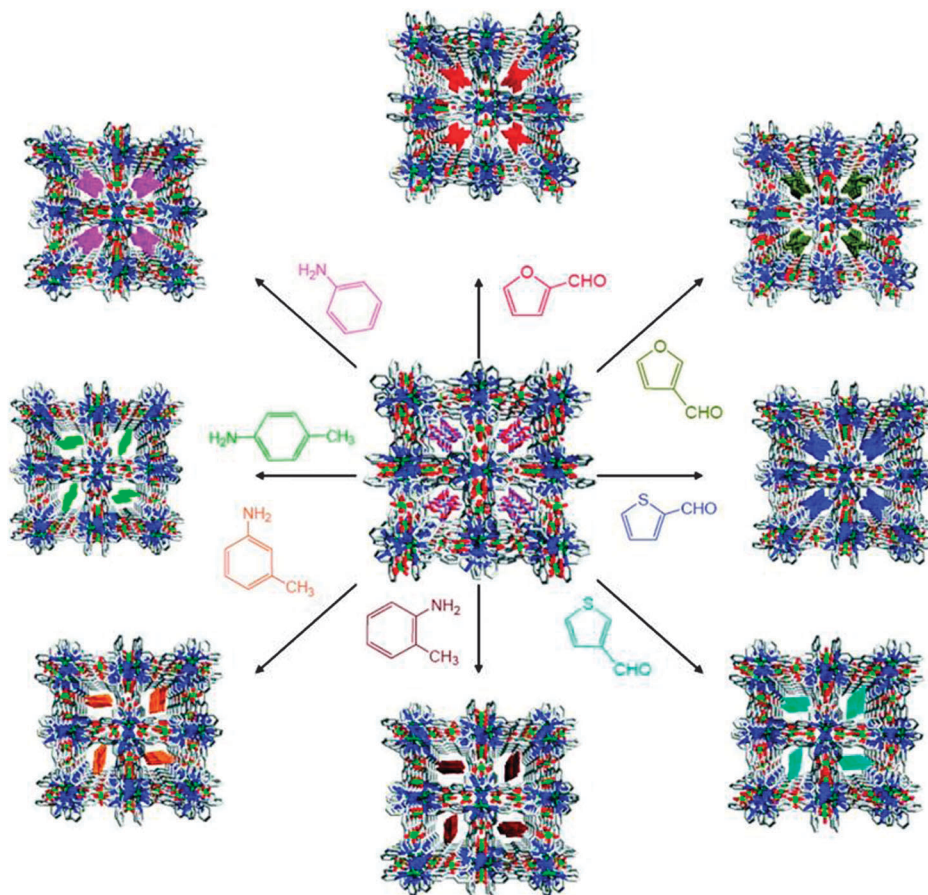**Fig. 23** Schematic representation of molecule encapsulations in $\{[Cd(ClO_4)_2(L)_2] \cdot H_2O\}_n$ based on the guest molecule substitutions. Reprinted with permission from ref. 221. Copyright 2010 American Chemical Society.

phase $\{[Cd(ClO_4)_2(L)_2] \cdot H_2O\}_n$, which could be used as a robust host for the reversible uptake and separation of benzene and its methyl- and halide-substituted derivatives *via* a SC–SC transformation.[220] Furthermore, this MOF also presented its ability in the encapsulation and separation of aromatic guest molecules with reactive functional groups.[221] As shown in Fig. 23, when the crystals of the hydrated MOF were exposed to 2-furaldehyde, 3-furaldehyde, 2-thiophenaldehyde, 3-thiophenaldehyde, *o*-toluidine, *m*-toluidine, *p*-toluidine, or aniline vapor at 50 °C for 4 days, it was revealed by SXRD analysis that all the original water molecules in the pores were substituted by these corresponding organic guests. It was also found that these guest molecules were stabilized in the MOF channels through hydrogen bonding interactions with the host framework and $ClO_4^-$ anions. In addition, it was confirmed that this MOF was capable of discerning and completely separating several functionalized aromatic isomers in both vapor and liquid phases, including 2-furaldehyde *vs.* 3-furaldehyde, 2-thiophenaldehyde *vs.* 3-thiophenaldehyde, and *o*-toluidine *vs. m*-toluidine *vs. p*-toluidine, under mild conditions.

In addition, structural transformations triggered by the guest molecule substitution have been observed in flexible/soft MOFs.[222] The first example in this context was reported by Lin and co-workers in a 1D compound $\{[CdL_2(ClO_4)_2] \cdot 11EtOH \cdot 6H_2O\}_n$

(L = (*S*)-2,2′-diethoxy-1,1′-binaphthyl-6,6′-bis(4-vinylpyridine)). The original crystal lost its crystallinity upon removal of guest molecules as confirmed by PXRD. However, the crystallinity was restored when exposing the resulting amorphous material to a solvent vapor. More importantly, the compound remained crystalline throughout but exhibited SC–SC transformations along with the formation of different structures, during several guest solvent substitution processes.[223] Vittal and co-workers reported another structural transformation example in a 3D MOF $\{[Zn_2(BPEB)(OBC)_2] \cdot 2DMF \cdot H_2O\}_n$ (BPEB = 1,4-bis[2-(4-pyridyl)-ethenyl]benzene, $H_2OBC$ = 4,4′-oxybisbenzoic acid) triggered by the guest exchange.[224] It was found that this MOF could be converted into $\{[Zn_2(BPEB)(OBC)_2] \cdot 2H_2O\}_n$ in MeOH *via* the solvent exchange, accompanied by the transformation from *trans–cis–trans* to *trans–trans–trans* conformation of the BPEB ligand. And, the reversible conversion could be achieved by soaking $\{[Zn_2(BPEB)(OBC)_2] \cdot 2H_2O\}_n$ in DMF solvent.

On the other hand, some flexible MOFs also showed unique and interesting guest-induced structural transformation features, such as a "breathing" effect.[225] In these cases, the flexible frameworks were able to optimize their pore sizes and shapes in accordance with the incoming guest molecules. For example, Walton and co-workers observed a "breathing" effect in $\{Fe(OH,F)(BDC) \cdot H_2O\}_n$ (MIL-53(Fe), $H_2O$), which was induced
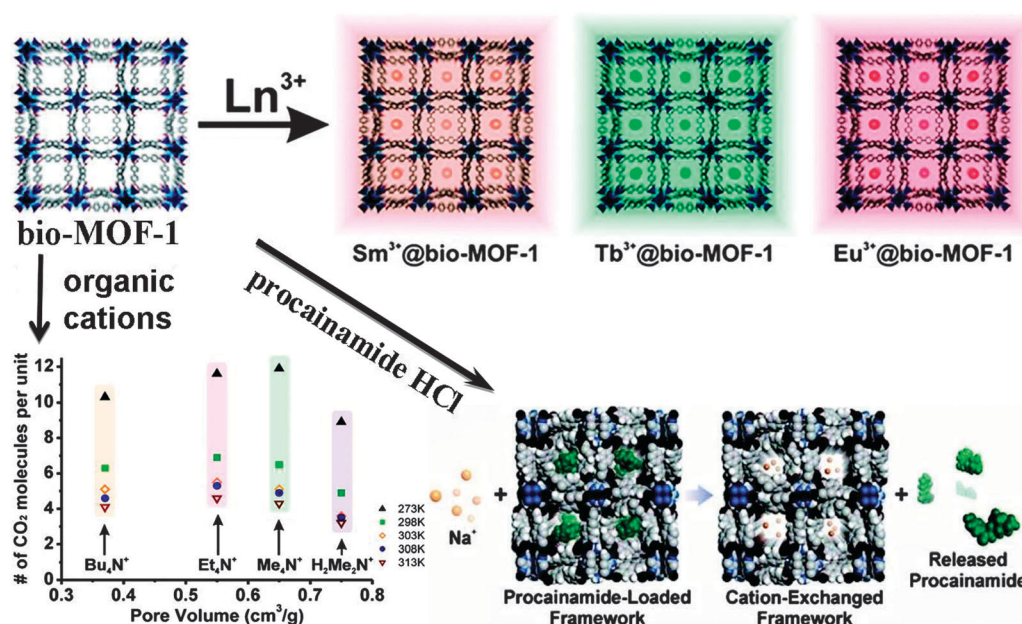
**Fig. 24** Schematic representation of applications of $\{[Me_2NH_2]_2[Zn_8(AD)_4(BPDC)_6O]\cdot8DMF\cdot11H_2O\}_n$ (bio-MOF-1) in drug delivery, $CO_2$ absorption, and lanthanide ion sensing, all based on the cation substitutions. Reprinted with permission from ref. 227–229. Copyright 2009, 2010 and 2011 American Chemical Society.

by the substitution of water molecules in the framework pores by a variety of organic molecules including methanol, acetonitrile, lutidine, pyridine, and *m*-xylene.[226] Interestingly, it was found that pyridine led to a small increase in the unit cell volume of the MOF, whereas lutidine gave the largest swelling. Particularly, a dramatic stepwise expansion–contraction of the framework was observed in the presence of different amounts of the guest molecules in each case.

## 4.2. Cationic guest molecule substitution

Cation substitution has also been explored in some MOFs with anionic framework skeletons. For example, Rosi and co-workers have shown potential applications of a MOF $\{[Me_2NH_2]_2$-$[Zn_8(AD)_4(BPDC)_6O]\cdot8DMF\cdot11H_2O\}_n$ (bio-MOF-1) in terms of its cation substitutions in drug delivery,[227] $CO_2$ separation,[228] and ion-dependent luminescence[229] (Fig. 24). The bio-MOF-1 has an anionic framework skeleton, with dimethylammonium (DMAM) counter cations residing in its pores. When the crystals of bio-MOF-1 were soaked in an antiarrhythmic drug-procainamide HCl solution for 15 days, a complete procainamide-loaded material $\{[procainamideH^+]_{3.5}[Zn_8(AD)_4(BPDC)_6O]\cdot1.5Cl\cdot16.5H_2O\}_n$ was obtained. Further studies showed that the release of the procainamide could be achieved by putting the inclusion sample in phosphate-buffered saline (PBS) buffer (pH 7.4). On the other hand, based on the cation exchange, the pore properties of bio-MOF-1 could be modified to give different gas adsorption performances of the resulting materials. It was confirmed that the incorporation of tetramethylammonium (TMAM), tetraethylammonium (TEAM), and tetrabutylammonium (TBAM) *via* the guest exchange with DMAM into the pores of this MOF resulted in a systematic decrease of the pore volume and surface area, but an enhanced $CO_2$ uptake of the resulting materials compared with

bio-MOF-1. This result demonstrated that small pores in MOFs might be better for preferentially adsorbing $CO_2$ molecules. In addition, bio-MOF-1 has also been used to encapsulate $Ln^{3+}$ ions through the cation substitution, to give a series of luminescent MOFs. Experimentally, $Ln^{3+}$@bio-MOF-1 materials were obtained *via* the substitution of DMAM with $Tb^{3+}$, $Sm^{3+}$, $Eu^{3+}$, or $Yb^{3+}$ by soaking bio-MOF-1 crystals in DMF solutions of the corresponding lanthanide nitrate salts. The DMF molecules in the pores were then washed with water. It was found that despite the strong quenching effect of the water molecules located in their pores, these $Ln^{3+}$@bio-MOF-1 materials emitted distinctive colors, $Eu^{3+}$, red; $Tb^{3+}$, green; $Sm^{3+}$, orange-pink, when excited with a 365 nm light. The bio-MOF-1 can thus be used as a sensing material to identify different lanthanide ions.

Furthermore, Ma and co-workers also developed a "two-step" approach to encapsulate larger metal(II) phthalocyanine molecules into bio-MOF-1.[230] In the first step, metal ions were introduced into the MOF pores through the cationic substitution. And then, in the second step the metal functionalized molecules were generated in the pores by the *de novo* assembly of the metal ions and the incoming small molecule reactant (for synthesizing phthalocyanine). This work demonstrated a new strategy to encapsulate large metal-functionalized guest molecules into MOFs for various applications.

Apart from luminescence, tuned nonlinear optical responses have been observed in MOFs based on the cation substitutions. The MOF $\{[DMAM]_3[In_3(BTB)_4]\cdot12DMF\cdot22H_2O\}_n$ (ZJU-28) reported by Chen and co-workers did not present a second order nonlinear optical response.[231] The substitution of DMAM in this MOF with different hemicyanine chromophores of 4-(4-(diphenylamino)styryl)-1-methylpyridinium (DPASM), 1-butyl-4-(4-(diphenylamino)styryl)pyridinium (DPASB), 4-(4-(diphenylamino)styryl)-1-nonylpyridinium
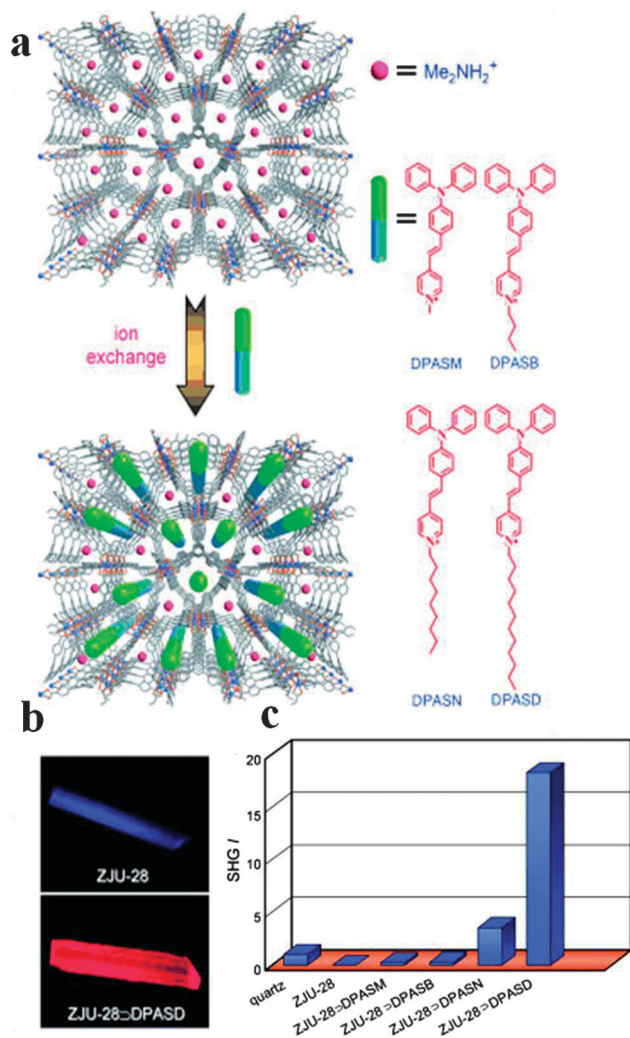
**Fig. 25** (a) Schematic representation of the incorporation of pyridinium hemicyanine chromophores into $\{[DMAM]_3[In_3(BTB)_4]\cdot 12DMF\cdot 22H_2O\}_n$ (ZJU-28) *via* cation substitutions. (b) Fluorescence microscope images of ZJU-28 and ZJU-28⊃DPASD illuminated with a 365 nm UV light. (c) Comparison of the SHG intensities of α-quartz, ZJU-28, and the chromophore-substituted ZJU-28. Reprinted with permission from ref. 231. Copyright 2012 WILEY-VCH Verlag GmbH & Co. KGaA, Weinheim.

(DPASN), or 4-(4-(diphenylamino)styryl)-1-dodecylpyridinium (DPASD) containing different lengths of alkyl chains in DMF solution resulted in nonlinear optically respondent MOF materials: ZJU-28⊃DPASM, ZJU-28⊃DPASB, ZJU-28⊃DPASN, and ZJU-28⊃DPASD, respectively (Fig. 25). Second harmonic generation (SHG) measurements indicated that the longer the terminal alkyl chain of the chromophore guest ion, the stronger the SHG intensity of the resulting MOF material. This observation was explained as that the included chromophore guest ions with longer alkyl chains might get the maximum match with the 1D channels of the MOF, which thus enhanced their interactions with the host framework to give stronger SHG intensity. In addition, the luminescence properties of these materials also changed after the cation substitutions. For instance, when excited at 365 nm, ZJU-28 displayed a blue light emission at 414 nm, whereas ZJU-28⊃DPASD showed a red

emission at 634 nm. Thereafter, through the cationic guest exchange, a very unique MOF material for lasing application has been realized by the same group.[232] The confinement of pyridinium hemicyanine dye 4-[p-(dimethylamino)styryl]-1-methylpyridinium (DMASM) within the anionic bio-MOF-1 produced the bio-MOF-1⊂DMASM composite. This material exhibited two-photon fluorescence on account of the large absorption cross-section and the enhanced luminescence efficiency of the encapsulated DMASM. More importantly, the MOF composite crystal can serve as a Fabry–Perot resonance cavity to give rise to two-photon-pumped lasing around 640 nm when pumped with a 1064 nm pulse laser.

The cation substitution has also been proved to be a powerful method for tuning the gas adsorption properties of MOFs, such as in $H_2$ storage.[233–235] $Li^+$-doped MOFs have received considerable attention due to the strong $Li^+\cdots H_2$ interactions involved and thereby their high $H_2$ storage ability. In several reported examples, $Li^+$ ions were introduced into the pores of MOFs through the cation substitution to get materials with enhanced $H_2$ adsorption ability.[236–240] For instance, Schröder and co-workers reported the $Li^+$ exchange in $\{[H_2PPZ][In_2(L^1)_2]\cdot 3.5DMF\cdot 5H_2O\}_n$ (NOTT-200; $L^1 = 1,1',4',1'',4'',1'''$-quaterphenyl-$3,5,3''',5'''$-tetracarboxylate, PPZ = piperazine), which has a 2-fold interpenetrated anionic framework containing three interlinked channels (A, B, and C) as illustrated in Fig. 26.[241] In the structure, $H_2PPZ^{2+}$ cations are fully ordered and located in the centre of channel B. The crystals of NOTT-200 were immersed in a saturated solution of LiCl in water–acetone at room temperature to give the expected $Li^+$-exchanged MOF, $\{Li_{1.5}[H_3O]_{0.5}[In_2(L)_2]\cdot 11H_2O\}_n$ (NOTT-201). It was found that in NOTT-201 the $Li^+$ ions located in channel C and were tetrahedrally coordinated by two water molecules and two O atoms from carboxylate groups of the $L^1$ ligands. After removal of the coordinated water molecules, the $Li^+$ sites were exposed to give the material a greatly enhanced $H_2$ adsorption ability. Before and after the cation exchange, both MOFs indeed showed different gas adsorption behaviors: NOTT-200 showed a significant kinetic hysteresis for $N_2$ and $H_2$ adsorption, whereas NOTT-201 exhibited no hysteresis but a higher isosteric heat of adsorption towards $H_2$.

The same group also reported similar examples based on another two isostructural MOFs $\{[(DMAM)(H_3O)][In_2(L^2)_2]_3\cdot 4DMF\cdot 5H_2O\}_n$
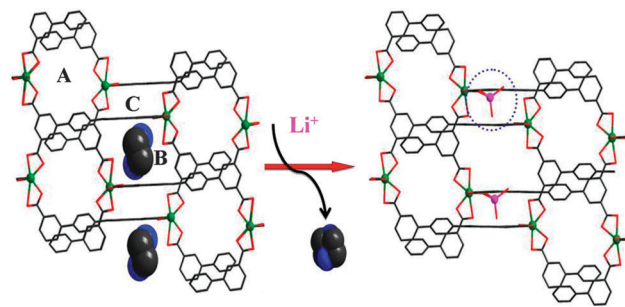


**Fig. 26** Schematic representation of the substitution of $H_2PPZ^{2+}$ cations in $\{[H_2PPZ][In_2(L^1)_2]\cdot 3.5DMF\cdot 5H_2O\}_n$ (NOTT-201) by $Li^+$ ions to form $\{Li_{1.5}[H_3O]_{0.5}[In_2(L)_2]\cdot 11H_2O\}_n$ (NOTT-201).[241]

This journal is © The Royal Society of Chemistry 2014

*Chem. Soc. Rev.*, 2014, **43**, 5952–5981 | **5973**

(NOTT-206-solv, $L^2$ = 5,5′-(9,10-dihydrophenanthrene-2,7-diyl)diisophthalate) and $\{[H_2PPZ][In_2(L^3)_2]\cdot4DMF\cdot5.5H_2O\}_n$ (NOTT-208-solv, $L^3$ = 1,1′,4′,1″,4″,1‴-quinquephenyl-3,5,3‴,5‴-tetracarboxylate), in which organic cations were replaced by $Li^+$ ions to yield the corresponding $Li^+$-containing MOFs $\{Li_{1.2}[H_3O]_{0.8}[In_2(L^2)_2]\cdot14H_2O\}_n$ (NOTT-207-solv) and $\{Li_{1.4}[H_3O]_{0.6}[In_2(L^3)_2]\cdot4acetone\cdot11H_2O\}_n$ (NOTT-209-solv).[242] After the substitution, a remarkable enhancement in $H_2$ storage capacity with the increased isosteric heat of adsorption was achieved in each case.

Another interesting example was the observation of the coordination of incoming metal ions after the cation substitution to give a new MOF, a transformation from an anionic framework MOF to a neutral bimetallic one, reported by Thallapally and co-workers.[243] It was demonstrated that immersing the crystals of anionic framework MOF $\{[DMAM]_2[Mn_3(L)_2]\cdot9DMF\}_n$ ($H_4L$ = tetrakis[4-(carboxyphenyl)oxamethyl]-methane acid) in a DMF solution of $M(NO_3)_2$ (M = Co, Ni, or Cu) produced the corresponding neutral heterobimetallic MOFs via a SC–SC transformation process (Fig. 27) where DMAM cations in the parent MOF were substituted by metal ions. Different from most of the observed guest molecule substitutions, these transformations were accompanied by breakage and regeneration of coordination bonds, being quite interesting in MOF chemistry. It was also found that $Co^{2+}$ and $Ni^{2+}$ ions could be selectively taken up over $Li^+$ and $Na^+$ ions by this MOF based on the cation substitution. This MOF is thus potentially useful for the removal of heavy metal ions from some complex solution systems.

## 4.3. Anionic guest molecule substitution

Similar to the cation substitution, anion substitution has also been observed and explored in MOFs and MOPs for tuning their properties.[244,245] When using a neutral organic ligand to



Fig. 27 Schematic representation of the cation substitution of organic DMAM by $M^{2+}$ ions in anionic $\{[DMAM]_2[Mn_3(L)_2]\cdot9DMF\}_n$ to afford a neutral MOF (top). Photographs of a crystal before and after the cationic guest exchange in the MOF (bottom). Reprinted with permission from ref. 243. Copyright 2012 American Chemical Society.

coordinate with metal ions, the resulting MOFs usually have a cationic framework with uncoordinated anions balancing the charge. In the early state of MOF development, a lot of these MOFs were synthesized, where the free anions can be substituted by others. Some examples have been reported, mostly for exploring the potential applications of these MOFs such as in pollution removal and molecule adsorption.[246]

For example, Oliver and co-workers studied the anion exchange in two cationic framework MOFs $\{Ag_2(BIPY)_2(EDS)\}_n$ (SLUG-21; EDS = 1,2-ethanedisulfonate)[247] and $\{Cu_2(BIPY)_2(EDS)\}_n$ (SLUG-22),[248] in which the $Cu^+$- or $Ag^+$-BIPY chains were held together via $\pi\cdots\pi$ stacking to form cationic layers. EDS anions located between the layers and formed weak coordination interactions with $Cu^+$ or $Ag^+$ ions. It was found that immersing SLUG-21 crystals in an aqueous solution of $NaNO_3$ at room temperature produced complete $NO_3^-$-exchanged product $[Ag(BIPY)_2(NO_3)]_n$ (SLUG-21-$NO_3$[249]), and the substitution process was reversible under similar conditions. In addition to the $NO_3^-$ substitution, SLUG-21 also showed a reversible substitution towards $ClO_4^-$, but irreversible towards $MnO_4^-$. Similarly, SLUG-22 exhibited the same anion exchange properties with $NO_3^-$ and $ClO_4^-$. Furthermore, a selective anion exchange of $MnO_4^-$ over $NO_3^-$ was also observed in SLUG-21. It was found that $MnO_4^-$ could preferably substitute EDS and form stronger interactions with the SLUG-21 cationic framework than $NO_3^-$, which explained the observed irreversible exchange in the $MnO_4^-$ case. The preferable substitution was also observed for $ClO_4^-$ over $NO_3^-$, and $ReO_4^-$ over $NO_3^-$ and $CO_3^{2-}$.[250] The same group also reported the anion substitution in another MOF $\{[Pb_2F_2][EDS]\}_n$ (SLUG-6) consisting of cationic $[Pb_2F_2]^{2+}$ layers pillared by EDS anions (Fig. 28).[251] It was found that the immersion of SLUG-6 crystals in an aqueous solution of excess disodium succinate under ambient conditions gave crystalline $\{[Pb_2F_2][succinate]\}_n$ (SLUG-32). In situ optical microscopy analysis indicated that SLUG-6 underwent a solvent-mediated anion exchange, probably a dissolution and recrystallization process. Similarly, longer dicarboxylate ligands, such as glutarate and sebacate, have also been confirmed to be able to substitute EDS in SLUG-6 to produce new MOFs with a similar structure.[252]

Another example of anion exchange was reported by Wang and co-workers on the MOF $\{[Ag_2(BTR)_2]\cdot2ClO_4\cdot3H_2O\}_n$ (BTR = 4,4′-bis(1,2,4-triazole)) with 1D channels, which were filled by $ClO_4^-$ anions.[253] Immersing colorless crystals of this MOF in an aqueous solution of $K_2Cr_2O_7$ produced the orange yellow crystals of $Cr_2O_7^{2-}$ loaded MOF. SXRD analysis indicated that $ClO_4^-$ anions in the parent MOF were completely exchanged by $Cr_2O_7^{2-}$ ions and the cationic framework was still intact. It was also found that this MOF presented a high substitution selectivity towards $Cr_2O_7^{2-}$ over $NO_3^-$, $CF_3SO_3^-$, and $BF_4^-$ ions, probably due to the stronger interactions of $Cr_2O_7^{2-}$ with the cationic framework than other anions. Interestingly, a bluish violet luminescence of $\{[Ag_2(BTR)_2]\cdot2ClO_4\}_n$ was quenched upon the $Cr_2O_7^{2-}$ exchange. It should be pointed out that a lot of pollutants occurred in an anionic form, such as $MnO_4^-$, $ClO_4^-$, $CrO_4^{2-}$, $Cr_2O_7^{2-}$, salicylate, carbamazepine, clofibrate, and ibuprofen. The above-mentioned examples show that MOFs
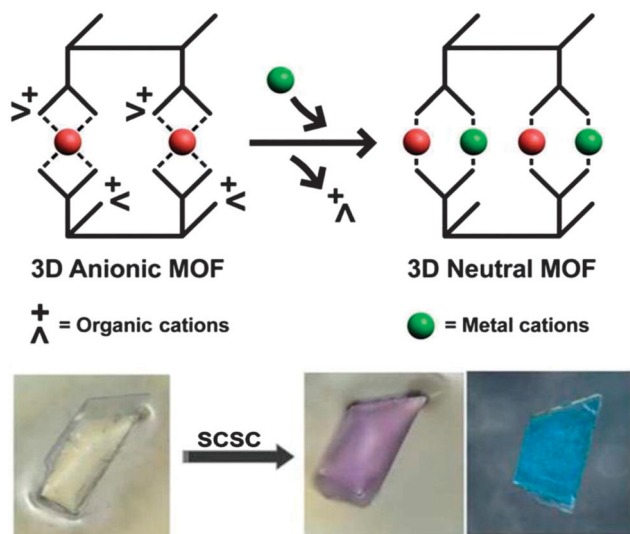
5974 | Chem. Soc. Rev., 2014, 43, 5952–5981
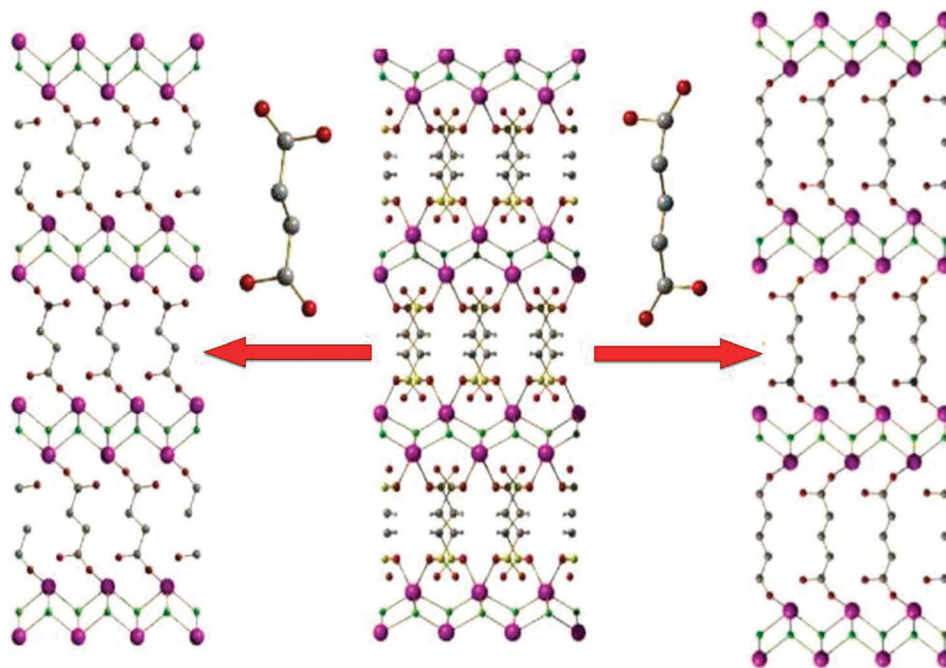
This journal is © The Royal Society of Chemistry 2014

**Fig. 28** Schematic representation of the guest anion substitutions in $\{[Pb_2F_2][EDS]\}_n$ (SLUG-6) to form new MOFs. Reprinted with permission from ref. 252. Copyright 2012 American Chemical Society.

with a cationic framework can potentially be applied for pollutant removal, even if only very limited MOFs have been explored to date in this aspect.

Based on the anion substitution some MOFs could also exhibit sensing responses towards given anions. For example, Kitagawa and co-workers reported the selective anion substitution in a 3D flexible MOF $\{[Ni(BPE)_2(N(CN)_2)]\cdot N(CN)_2\cdot 5H_2O\}_n$ (BPE = 1,2-bis(4-pyridyl)ethane, $N(CN)_2{}^-$ =dicyanamide), which can identify $N_3{}^-$ ions in terms of its color change.[254] When crystals of this MOF were immersed in an aqueous solution of excess $NaN_3$ for 1 day, a color change of the crystals from violet to light green was observed. Following characterizations confirmed that free $N(CN)_2{}^-$ anions in the MOF were completely substituted by $N_3{}^-$ ions to give $\{[Ni(BPE)_2(N(CN)_2)]\cdot N_3\cdot 5H_2O\}_n$. However, other anions including $NCO^-$, $NO_3{}^-$, $BF_4{}^-$, $ClO_4{}^-$, and $PF_6{}^-$ were not able to substitute $N(CN)_2{}^-$, showing the selectivity of this MOF towards different substituted anions. Interestingly, due to the decreased size of $N_3{}^-$ compared with the $N(CN)_2{}^-$ anion, the $N_3{}^-$ substitution led to a slight change of the structure and an increase in its channel size, and thereby an enhanced $CO_2$ uptake capacity of this MOF. In addition, the structural transformation triggered by the anion substitution in MOFs has also been observed. For example, Hou and co-workers presented a SC–SC transformation from $\{[Cu_6(TTTMB)_8(OH)_4(H_2O)_6]\cdot 8(NO_3)\}_n$ to $\{[Cu_6(TTTMB)_8I_3]\cdot 9I\}_n$ (TTTMB = 1,3,5-tris(triazol-1-ylmethyl)-2,4,6-trimethylbenzene) achieved by the replacement of guest $NO_3{}^-$ anions in the former with $I^-$,[255] where the coordination geometry of $Cu^{2+}$ ions in the MOF changed from octahedral to square-planar, accompanied by a visible color change of the crystals from light blue to dark blue.

Another colorimetric anion sensing was achieved in the MOF $\{[CuL_2(H_2O)_{0.5}](NO_3)_2\cdot 3.25(CH_2Cl_2)\cdot(CH_3OH)\cdot 0.5H_2O\}_n$ (L = 4,4′-(9,9-dibutyl-9H-fluorene-2,7-diyl)dipyridine) reported by Dong and co-workers.[256] As shown in Fig. 29, it was found that immersing the crystals of the MOF in an aqueous solution of NaF, NaCl, KBr, KI, KSCN, or $NaN_3$, respectively, resulted in a detectable color change in them. Different anions gave different colors of the resulting materials: green for $Cl^-$, dark green for $Br^-$, deep brown for $I^-$, blackish green for $SCN^-$, and tan for $N_3{}^-$. However, no color change was observed for $F^-$. In addition, this MOF was confirmed to be able to separate $Cl^-/Br^-$, $Br^-/I^-$, and $SCN^-/N_3{}^-$ anions under ambient conditions based on their selective substitutions.

It is clear that free guest molecules are usually stabilized in the cavities of MOMs *via* weak interactions. Compared with the relatively strong coordination bonds, such weak interactions
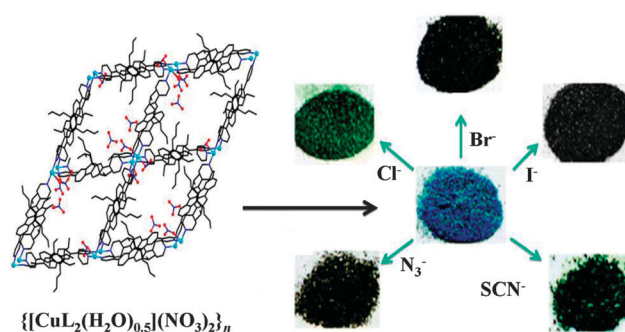


**Fig. 29** Crystal structure and color changes of $\{[CuL_2(H_2O)_{0.5}](NO_3)_2\cdot 3.25(CH_2Cl_2)\cdot(CH_3OH)\cdot 0.5H_2O\}_n$ resulting from anion substitutions. Reprinted with permission from ref. 256. Copyright 2012 The Royal Society of Chemistry.

This journal is © The Royal Society of Chemistry 2014

*Chem. Soc. Rev.*, 2014, **43**, 5952–5981 | **5975**

make guest molecules much easier to be substituted. And simultaneously, the substitution can also lead to some responses of the host framework towards the incoming guest molecules due to these weak interactions, to give unique phenomena, which are useful in several fields such as chemical sensing and reorganization. Thus, a lot of new structures or new properties of MOFs and MOPs can be achieved by the guest substitution strategy. In addition, we speculate that a lot of other new effects and/or applications are accessible in this context with the effort of further exploration in the future.

## 5. Conclusions and outlook

Metal–organic materials (MOMs) including MOFs and MOPs are a class of newly developed multifunctional materials with a wide range of potential applications. The synthesis and functional modifications of these materials are crucial for their applications. Compared with the efforts on the exploitation of suitable synthetic methods/conditions based on the usually used "one-pot" self-assembly strategy for preparing functional MOMs, the study of substitution reactions in MOMs for their preparation, modification, and transformation is still at the early stage, despite some examples being reported as discussed in this review.

Different from the traditional synthetic method, the preparation of MOMs *via* the substitution reaction at metal ions or organic ligands is mainly based on a process starting from a pre-designed framework template, which could lead to a desired functional structure that may be difficult to access through a direct construction strategy. A lot of examples have demonstrated that the substitution reaction is universal in MOMs, even in very "inert" ones. The substitution strategy is thus powerful and widely accessible for the synthesis and modification of MOMs. The occurrence of the substitution reaction suggests the dynamic feature of MOMs, which can be attributed to the nature of the coordination bond involved in all MOMs, that is "labile and reversible". Furthermore, the substitution/exchange of guest molecules can greatly enrich the MOMs' chemistry, as well as host–guest chemistry. Consequently, the substitution reaction in MOMs has a great potential and big space for further exploration.

However, reported examples in this topic mainly treated the structural transformations and associated property/function modifications induced by the substitution reactions mostly from experimental observations. An in-depth exploration of the mechanism, particularly the reaction rate, selectivity, and the relationship between structural transformations and resulting properties, needs to be carried out in the future, not only from experimental investigations but also from theoretical calculations based on molecular simulations. We are looking forward to a bright future for the substitution reaction application in MOFs and MOPs.

## Acknowledgements

## References

1  R. Xu, W. Pang, J. Yu, Q. Huo and J. Chen, *Chemistry of Zeolites and Related Porous Materials Synthesis and Structure*, Wiley, Singapore, 2007.

2  D. W. Beck, *Zeolite Molecular Sieves*, John Wiley & Sons, New York, 1974.

3  S. M. Auerbach, K. A. Carrado and P. K. Dutta, *Handbook of Zeolite Science and Technology*, Marcel Dekker, Inc., New York, 2003.

4  F. Schuth, K. S. W. Sing and J. Weitkamp, *Handbook of Porous Solids*, Wiley-VCH, New York, 2002.

5  S.-Y. Ding and W. Wang, *Chem. Soc. Rev.*, 2013, **42**, 548–568.

6  A. Lee, S. Dubinsky, E. Tumarkin, M. Moulin, A. A. Beharry and E. Kumacheva, *Adv. Funct. Mater.*, 2011, **21**, 1959–1969.

7  G. Férey, *Chem. Soc. Rev.*, 2008, **37**, 191–214.

8  H.-C. Zhou, J. R. Long and O. M. Yaghi, *Chem. Rev.*, 2012, **112**, 673–674.

9  J. R. Long and O. M. Yaghi, *Chem. Soc. Rev.*, 2009, **38**, 1213–1214.

10  T. R. Cook, Y.-R. Zheng and P. J. Stang, *Chem. Rev.*, 2013, **113**, 734–777.

11  R. Chakrabarty, P. S. Mukherjee and P. J. Stang, *Chem. Rev.*, 2011, **111**, 6810–6918.

12  H. Furukawa, K. E. Cordova, M. O'Keeffe and O. M. Yaghi, *Science*, 2013, **341**, 1230444.

13  C. Wang, D. Liu and W. Lin, *J. Am. Chem. Soc.*, 2013, **135**, 13222–13234.

14  T. A. Makal, J.-R. Li, W. Lu and H.-C. Zhou, *Chem. Soc. Rev.*, 2012, **41**, 7761–7779.

15  M. P. Suh, H. J. Park, T. K. Prasad and D. W. Lim, *Chem. Rev.*, 2012, **112**, 782–835.

16  D. M. D'Alessandro, B. Smit and J. R. Long, *Angew. Chem., Int. Ed.*, 2010, **49**, 6058–6082.

17  J.-R. Li, J. Sculley and H.-C. Zhou, *Chem. Rev.*, 2012, **112**, 869–932.

18  J.-R. Li, R. J. Kuppler and H.-C. Zhou, *Chem. Soc. Rev.*, 2009, **38**, 1477–1504.

19  K. Sumida, D. L. Rogow, J. A. Mason, T. M. McDonald, E. D. Bloch, Z. R. Herm, T. H. Bae and J. R. Long, *Chem. Rev.*, 2012, **112**, 724–781.

20  Z. Zhang, Y. Zhao, Q. Gong, Z. Li and J. Li, *Chem. Commun.*, 2013, **49**, 653–661.

21  L. Ma, C. Abney and W. Lin, *Chem. Soc. Rev.*, 2009, **38**, 1248–1256.

22  J. Lee, O. K. Farha, J. Roberts, K. A. Scheidt, S. T. Nguyen and J. T. Hupp, *Chem. Soc. Rev.*, 2009, **38**, 1450–1459.

23  M. Yoon, R. Srirambalaji and K. Kim, *Chem. Rev.*, 2012, **112**, 1196–1231.

24  L. E. Kreno, K. Leong, O. K. Farha, M. Allendorf, R. P. Van Duyne and J. T. Hupp, *Chem. Rev.*, 2012, **112**, 1105–1125.

25  B. Chen, S. Xiang and G. Qian, *Acc. Chem. Res.*, 2010, **43**, 1115–1124.

26  Y. Cui, Y. Yue, G. Qian and B. Chen, *Chem. Rev.*, 2012, **112**, 1126–1162.

27 P. Horcajada, R. Gref, T. Baati, P. K. Allan, G. Maurin, P. Couvreur, G. Férey, R. E. Morris and C. Serre, *Chem. Rev.*, 2012, **112**, 1232–1268.

28 J. Della Rocca, D. Liu and W. Lin, *Acc. Chem. Res.*, 2011, **44**, 957–968.

29 Z. Ma and B. Moulton, *Coord. Chem. Rev.*, 2011, **255**, 1623–1641.

30 J. J. Perry IV, J. A. Perman and M. J. Zaworotko, *Chem. Soc. Rev.*, 2009, **38**, 1400–1417.

31 N. Stock and S. Biswas, *Chem. Rev.*, 2012, **112**, 933–969.

32 D. Braga, S. L. Giaffreda, F. Grepioni, A. Pettersen, L. Maini, M. Curzi and M. Polito, *Dalton Trans.*, 2006, 1249–1263.

33 C.-P. Li and M. Du, *Chem. Commun.*, 2011, **47**, 5958–5972.

34 S. S. Nagarkar, A. K. Chaudhari and S. K. Ghosh, *Cryst. Growth Des.*, 2012, **12**, 572–576.

35 P. Mahata, M. Prabu and S. Natarajan, *Inorg. Chem.*, 2008, **47**, 8451–8463.

36 N. A. Khan, J. W. Jun and S. H. Jhung, *Eur. J. Inorg. Chem.*, 2010, 1043–1048.

37 I. A. Riddell, Y. R. Hristova, J. K. Clegg, C. S. Wood, B. Breiner and J. R. Nitschke, *J. Am. Chem. Soc.*, 2013, **135**, 2723–2733.

38 Z. Zhang, L. Zhang, L. Wojtas, M. Eddaoudi and M. J. Zaworotko, *J. Am. Chem. Soc.*, 2012, **134**, 928–933.

39 O. M. Yaghi, M. O'Keeffe, N. W. Ockwig, H. K. Chae, M. Eddaoudi and J. Kim, *Nature*, 2003, **423**, 705–714.

40 D. J. Tranchemontagne, Z. Ni, M. O'Keeffe and O. M. Yaghi, *Angew. Chem., Int. Ed.*, 2008, **47**, 5136–5147.

41 J. B. Rivest and P. K. Jain, *Chem. Soc. Rev.*, 2013, **42**, 89–96.

42 R. J. Puddephatt, *Chem. Soc. Rev.*, 2008, **37**, 2012–2027.

43 D. T. Richens, *Chem. Rev.*, 2005, **105**, 1961–2002.

44 M. Lalonde, W. Bury, O. Karagiaridi, Z. Brown, J. T. Hupp and O. K. Farha, *J. Mater. Chem. A*, 2013, **1**, 5453–5468.

45 M. E. Carnes, M. S. Collins and D. W. Johnson, *Chem. Soc. Rev.*, 2014, **43**, 1825–1834.

46 B. J. Burnett and W. Choe, *Dalton Trans.*, 2012, **41**, 3889–3894.

47 G. K. Kole and J. J. Vittal, *Chem. Soc. Rev.*, 2013, **42**, 1755–1775.

48 M. Kim, J. F. Cahill, H. Fei, K. A. Prather and S. M. Cohen, *J. Am. Chem. Soc.*, 2012, **134**, 18082–18088.

49 H. Fei, J. F. Cahill, K. A. Prather and S. M. Cohen, *Inorg. Chem.*, 2013, **52**, 4011–4016.

50 O. Karagiaridi, W. Bury, A. A. Sarjeant, C. L. Stern, O. K. Farha and J. T. Hupp, *Chem. Sci.*, 2012, **3**, 3256–3260.

51 M. Kim, J. F. Cahill, Y. Su, K. A. Prather and S. M. Cohen, *Chem. Sci.*, 2012, **3**, 126–130.

52 G. Férey, C. Mellot-Draznieks, C. Serre, F. Millange, J. Dutour, S. Surble and I. Margiolaki, *Science*, 2005, **309**, 2040–2042.

53 J. J. Vittal, *Coord. Chem. Rev.*, 2007, **251**, 1781–1795.

54 S. Neogi, S. Sen and P. K. Bharadwaj, *CrystEngComm*, 2013, **15**, 9239–9248.

55 G. J. Halder and C. J. Kepert, *Aust. J. Chem.*, 2006, **59**, 597–604.

56 S. M. Cohen, *Chem. Rev.*, 2012, **112**, 970–1000.

57 S. M. Cohen, *Chem. Sci.*, 2010, **1**, 32–36.

58 Z. Wang and S. M. Cohen, *Chem. Soc. Rev.*, 2009, **38**, 1315–1329.

59 K. K. Tanabe and S. M. Cohen, *Chem. Soc. Rev.*, 2011, **40**, 498–519.

60 H. Li, M. Eddaoudi, M. O'Keeffe and O. M. Yaghi, *Nature*, 1999, **402**, 276–279.

61 M. O'Keeffe and O. M. Yaghi, *Chem. Rev.*, 2012, **112**, 675–702.

62 D. J. Tranchemontagne, J. L. Mendoza-Cortes, M. O'Keeffe and O. M. Yaghi, *Chem. Soc. Rev.*, 2009, **38**, 1257–1283.

63 Y. Han, N. F. Chilton, M. Li, C. Huang, H. Xu, H. Hou, B. Moubaraki, S. K. Langley, S. R. Batten, Y. Fan and K. S. Murray, *Chem. – Eur. J.*, 2013, **19**, 6321–6328.

64 G. Mukherjee and K. Biradha, *Chem. Commun.*, 2012, **48**, 4293–4295.

65 M. Dincă and J. R. Long, *J. Am. Chem. Soc.*, 2007, **129**, 11172–11176.

66 M. Dincă, A. Dailly, Y. Liu, C. M. Brown, D. A. Neumann and J. R. Long, *J. Am. Chem. Soc.*, 2006, **128**, 16876–16883.

67 L. Mi, H. Hou, Z. Song, H. Han and Y. Fan, *Chem. – Eur. J.*, 2008, **14**, 1814–1821.

68 L. Mi, H. Hou, Z. Song, H. Han, H. Xu, Y. Fan and S.-W. Ng, *Cryst. Growth Des.*, 2007, **7**, 2553–2561.

69 J. Li, L. Li, H. Hou and Y. Fan, *Cryst. Growth Des.*, 2009, **9**, 4504–4513.

70 J.-A. Zhao, L. Mi, J. Hu, H. Hou and Y. Fan, *J. Am. Chem. Soc.*, 2008, **130**, 15222–15223.

71 X.-J. Wang, P.-Z. Li, L. Liu, Q. Zhang, P. Borah, J. D. Wong, X. X. Chan, G. Rakesh, Y. Li and Y. Zhao, *Chem. Commun.*, 2012, **48**, 10286–10288.

72 Z.-J. Zhang, W. Shi, Z. Niu, H.-H. Li, B. Zhao, P. Cheng, D.-Z. Liao and S.-P. Yan, *Chem. Commun.*, 2011, **47**, 6425–6427.

73 C. K. Brozek and M. Dincă, *Chem. Sci.*, 2012, **3**, 2110–2113.

74 H. Li, W. Shi, K. Zhao, H. Li, Y. Bing and P. Cheng, *Inorg. Chem.*, 2012, **51**, 9200–9207.

75 J. A. Botas, G. Calleja, M. Sanchez-Sanchez and M. G. Orcajo, *Langmuir*, 2010, **26**, 5300–5303.

76 C. K. Brozek and M. Dincă, *J. Am. Chem. Soc.*, 2013, **135**, 12886–12891.

77 C. K. Brozek, A. F. Cozzolino, S. J. Teat, Y.-S. Chen and M. Dincă, *Chem. Mater.*, 2013, **25**, 2998–3002.

78 D. Denysenko, M. Grzywa, M. Tonigold, B. Streppel, I. Krkljus, M. Hirscher, E. Mugnaioli, U. Kolb, J. Hanss and D. Volkmer, *Chem. – Eur. J.*, 2011, **17**, 1837–1848.

79 D. Denysenko, T. Werner, M. Grzywa, A. Puls, V. Hagen, G. Eickerling, J. Jelic, K. Reuter and D. Volkmer, *Chem. Commun.*, 2012, **48**, 1236–1238.

80 S. Biswas, M. Grzywa, H. P. Nayek, S. Dehnen, I. Senkovska, S. Kaskel and D. Volkmer, *Dalton Trans.*, 2009, 6487–6495.

81 S. Das, H. Kim and K. Kim, *J. Am. Chem. Soc.*, 2009, **131**, 3814–3815.

82 Y. Kim, S. Das, S. Bhattacharya, S. Hong, M. G. Kim, M. Yoon, S. Natarajan and K. Kim, *Chem. – Eur. J.*, 2012, **18**, 16642–16648.

This journal is © The Royal Society of Chemistry 2014

*Chem. Soc. Rev.*, 2014, **43**, 5952–5981 | **5977**

83  J.-H. Liao, W.-T. Chen, C.-S. Tsai and C.-C. Wang, *CrystEng-Comm*, 2013, **15**, 3377–3384.

84  Q. Yao, J. Sun, K. Li, J. Su, M. V. Peskov and X. Zou, *Dalton Trans.*, 2012, **41**, 3953–3955.

85  H. Irving and R. J. P. Williams, *J. Chem. Soc.*, 1953, 3192–3210.

86  Z. Wei, W. Lu, H.-L. Jiang and H.-C. Zhou, *Inorg. Chem.*, 2013, **52**, 1164–1166.

87  T. K. Prasad, D. H. Hong and M. P. Suh, *Chem. – Eur. J.*, 2010, **16**, 14043–14050.

88  Z. Zhang, L. Zhang, L. Wojtas, P. Nugent, M. Eddaoudi and M. J. Zaworotko, *J. Am. Chem. Soc.*, 2012, **134**, 924–927.

89  X. Song, T. K. Kim, H. Kim, D. Kim, S. Jeong, H. R. Moon and M. S. Lah, *Chem. Mater.*, 2012, **24**, 3065–3073.

90  X. Song, S. Jeong, D. Kim and M. S. Lah, *CrystEngComm*, 2012, **14**, 5753.

91  G. Férey, C. Serre, C. Mellot-Draznieks, F. Millange, S. Surble, J. Dutour and I. Margiolaki, *Angew. Chem., Int. Ed.*, 2004, **43**, 6296–6301.

92  C. Volkringer, M. Meddouri, T. Loiseau, N. Guillou, J. Marrot, G. Férey, M. Haouas, F. Taulelle, N. Audebrand and M. Latroche, *Inorg. Chem.*, 2008, **47**, 11892–11901.

93  K. Barthelet, J. Marrot, G. Férey and D. Riou, *Chem. Commun.*, 2004, 520–521.

94  J. H. Cavka, S. Jakobsen, U. Olsbye, N. Guillou, C. Lamberti, S. Bordiga and K. P. Lillerud, *J. Am. Chem. Soc.*, 2008, **130**, 13850–13851.

95  H. Hayashi, A. P. Cote, H. Furukawa, M. O'Keeffe and O. M. Yaghi, *Nat. Mater.*, 2007, **6**, 501–506.

96  J.-P. Zhang, Y.-B. Zhang, J.-B. Lin and X.-M. Chen, *Chem. Rev.*, 2012, **112**, 1001–1033.

97  K. S. Park, Z. Ni, A. P. Cote, J. Y. Choi, R. Huang, F. J. Uribe-Romo, H. K. Chae, M. O'Keeffe and O. M. Yaghi, *Proc. Natl. Acad. Sci. U. S. A.*, 2006, **103**, 10186–10191.

98  S. Biswas, T. Ahnfeldt and N. Stock, *Inorg. Chem.*, 2011, **50**, 9518–9526.

99  T. Devic, P. Horcajada, C. Serre, F. Salles, G. Maurin, B. Moulin, D. Heurtaux, G. Clet, A. Vimont, J.-M. Grenèche, B. L. Ouay, F. Moreau, E. Magnier, Y. Filinchuk, J. Marrot, J.-C. Lavalley, M. Daturi and G. Férey, *J. Am. Chem. Soc.*, 2009, **132**, 1127–1136.

100  M. Dan-Hardi, C. Serre, T. Frot, L. Rozes, G. Maurin, C. Sanchez and G. Férey, *J. Am. Chem. Soc.*, 2009, **131**, 10857–10859.

101  C. H. Hendon, D. Tiana, M. Fontecave, C. Sanchez, L. D'Arras, C. Sassoye, L. Rozes, C. Mellot-Draznieks and A. Walsh, *J. Am. Chem. Soc.*, 2013, **135**, 10942–10945.

102  R. P. Lively, M. E. Dose, J. A. Thompson, B. A. McCool, R. R. Chance and W. J. Koros, *Chem. Commun.*, 2011, **47**, 8667–8669.

103  Z. Zhang, L. Wojtas, M. Eddaoudi and M. J. Zaworotko, *J. Am. Chem. Soc.*, 2013, **135**, 5982–5985.

104  G. Kumar and R. Gupta, *Chem. Soc. Rev.*, 2013, **42**, 9403–9453.

105  J. M. Falkowski, C. Wang, S. Liu and W. Lin, *Angew. Chem., Int. Ed.*, 2011, **50**, 8674–8678.

106  Z. Xie, L. Ma, K. E. deKrafft, A. Jin and W. Lin, *J. Am. Chem. Soc.*, 2009, **132**, 922–923.

107  R. Kitaura, G. Onoyama, H. Sakamoto, R. Matsuda, S.-i. Noro and S. Kitagawa, *Angew. Chem., Int. Ed.*, 2004, **43**, 2684–2687.

108  B. Chen, X. Zhao, A. Putkham, K. Hong, E. B. Lobkovsky, E. J. Hurtado, A. J. Fletcher and K. M. Thomas, *J. Am. Chem. Soc.*, 2008, **130**, 6411–6423.

109  X.-S. Wang, L. Meng, Q. Cheng, C. Kim, L. Wojtas, M. Chrzanowski, Y.-S. Chen, X.-P. Zhang and S. Ma, *J. Am. Chem. Soc.*, 2011, **133**, 16322–16325.

110  X.-L. Yang, M.-H. Xie, C. Zou, Y. He, B. Chen, M. O'Keeffe and C.-D. Wu, *J. Am. Chem. Soc.*, 2012, **134**, 10638–10645.

111  D. Feng, H.-L. Jiang, Y.-P. Chen, Z.-Y. Gu, Z. Wei and H.-C. Zhou, *Inorg. Chem.*, 2013, **52**, 12661–12667.

112  D. Feng, W.-C. Chung, Z. Wei, Z.-Y. Gu, H.-L. Jiang, Y.-P. Chen, D. J. Darensbourg and H.-C. Zhou, *J. Am. Chem. Soc.*, 2013, **135**, 17105–17110.

113  P. Hambright, in *The Porphyrin Handbook*, ed. K. M. Kadish, K. M. Smith and R. Guilard, Academic Press, New York, 2000.

114  X.-S. Wang, M. Chrzanowski, L. Wojtas, Y.-S. Chen and S. Ma, *Chem. – Eur. J.*, 2013, **19**, 3297–3301.

115  X.-S. Wang, M. Chrzanowski, W.-Y. Gao, L. Wojtas, Y.-S. Chen, M. J. Zaworotko and S. Ma, *Chem. Sci.*, 2012, **3**, 2823–2827.

116  D. Feng, Z.-Y. Gu, J.-R. Li, H.-L. Jiang, Z. Wei and H.-C. Zhou, *Angew. Chem., Int. Ed.*, 2012, **51**, 10307–10310.

117  W. Morris, B. Volosskiy, S. Demir, F. Gandara, P. L. McGrier, H. Furukawa, D. Cascio, J. F. Stoddart and O. M. Yaghi, *Inorg. Chem.*, 2012, **51**, 6443–6445.

118  Y. Chen, T. Hoang and S. Ma, *Inorg. Chem.*, 2012, **51**, 12600–12602.

119  M. J. Manos, E. J. Kyprianidou, G. S. Papaefstathiou and A. J. Tasiopoulos, *Inorg. Chem.*, 2012, **51**, 6308–6314.

120  J. E. Mondloch, W. Bury, D. Fairen-Jimenez, S. Kwon, E. J. DeMarco, M. H. Weston, A. A. Sarjeant, S. T. Nguyen, P. C. Stair, R. Q. Snurr, O. K. Farha and J. T. Hupp, *J. Am. Chem. Soc.*, 2013, **135**, 10294–10297.

121  P. Deria, J. E. Mondloch, E. Tylianakis, P. Ghosh, W. Bury, R. Q. Snurr, J. T. Hupp and O. K. Farha, *J. Am. Chem. Soc.*, 2013, **135**, 16801–16804.

122  P. Deria, W. Bury, J. T. Hupp and O. K. Farha, *Chem. Commun.*, 2014, **50**, 1965–1968.

123  A. Dhakshinamoorthy, M. Alvaro and H. Garcia, *Chem. Commun.*, 2012, **48**, 11275–11288.

124  E. D. Bloch, W. L. Queen, R. Krishna, J. M. Zadrozny, C. M. Brown and J. R. Long, *Science*, 2012, **335**, 1606–1610.

125  J. G. Vitillo, L. Regli, S. Chavan, G. Ricchiardi, G. Spoto, P. D. C. Dietzel, S. Bordiga and A. Zecchina, *J. Am. Chem. Soc.*, 2008, **130**, 8386–8396.

126  Q. Yang and C. Zhong, *J. Phys. Chem. B*, 2005, **110**, 655–658.

127  B. Supronowicz, A. Mavrandonakis and T. Heine, *J. Phys. Chem. C*, 2013, **117**, 14570–14578.

128  J. J. Gutiérrez-Sevillano, J. M. Vicent-Luna, D. Dubbeldam and S. Calero, *J. Phys. Chem. C*, 2013, **117**, 11357–11366.

129 M. J. Ingleson, R. Heck, J. A. Gould and M. J. Rosseinsky, *Inorg. Chem.*, 2009, **48**, 9986–9988.

130 M. Banerjee, S. Das, M. Yoon, H. J. Choi, M. H. Hyun, S. M. Park, G. Seo and K. Kim, *J. Am. Chem. Soc.*, 2009, **131**, 7524–7525.

131 Y. K. Hwang, D. Y. Hong, J. S. Chang, S. H. Jhung, Y. K. Seo, J. Kim, A. Vimont, M. Daturi, C. Serre and G. Férey, *Angew. Chem., Int. Ed.*, 2008, **47**, 4144–4148.

132 T. M. McDonald, W. R. Lee, J. A. Mason, B. M. Wiers, C. S. Hong and J. R. Long, *J. Am. Chem. Soc.*, 2012, **134**, 7056–7065.

133 A. Demessence, D. M. D'Alessandro, M. L. Foo and J. R. Long, *J. Am. Chem. Soc.*, 2009, **131**, 8784–8786.

134 H. J. Park, Y. E. Cheon and M. P. Suh, *Chem. – Eur. J.*, 2010, **16**, 11662–11669.

135 R. Kitaura, F. Iwahori, R. Matsuda, S. Kitagawa, Y. Kubota, M. Takata and T. C. Kobayashi, *Inorg. Chem.*, 2004, **43**, 6522–6524.

136 Z. Chen, S. Xiang, D. Zhao and B. Chen, *Cryst. Growth Des.*, 2009, **9**, 5293–5296.

137 M. Nagarathinam and J. J. Vittal, *Chem. Commun.*, 2008, 438–440.

138 M. Nagarathinam, A. Chanthapally, S. H. Lapidus, P. W. Stephens and J. J. Vittal, *Chem. Commun.*, 2012, **48**, 2585–2587.

139 A. Mallick, B. Garai, D. D. Diaz and R. Banerjee, *Angew. Chem., Int. Ed.*, 2013, **52**, 13755–13759.

140 M. J. Zaworotko, *Nat. Chem.*, 2009, **1**, 267–268.

141 T.-F. Liu, Y.-P. Chen, A. A. Yakovenko and H.-C. Zhou, *J. Am. Chem. Soc.*, 2012, **134**, 17358–17361.

142 J.-R. Li, D. J. Timmons and H.-C. Zhou, *J. Am. Chem. Soc.*, 2009, **131**, 6368–6369.

143 H.-N. Wang, X. Meng, G.-S. Yang, X.-L. Wang, K.-Z. Shao, Z.-M. Su and C.-G. Wang, *Chem. Commun.*, 2011, **47**, 7128–7130.

144 H. Furukawa, J. Kim, N. W. Ockwig, M. O'Keeffe and O. M. Yaghi, *J. Am. Chem. Soc.*, 2008, **130**, 11650–11661.

145 X.-L. Wang, C. Qin, S.-X. Wu, K.-Z. Shao, Y.-Q. Lan, S. Wang, D.-X. Zhu, Z.-M. Su and E.-B. Wang, *Angew. Chem., Int. Ed.*, 2009, **48**, 5291–5295.

146 Y.-Q. Lan, S.-L. Li, H.-L. Jiang and Q. Xu, *Chem. – Eur. J.*, 2012, **18**, 8076–8083.

147 A. Schoedel, L. Wojtas, S. P. Kelley, R. D. Rogers, M. Eddaoudi and M. J. Zaworotko, *Angew. Chem., Int. Ed.*, 2011, **50**, 11421–11424.

148 A. Schoedel, A. J. Cairns, Y. Belmabkhout, L. Wojtas, M. Mohamed, Z. Zhang, D. M. Proserpio, M. Eddaoudi and M. J. Zaworotko, *Angew. Chem., Int. Ed.*, 2013, **52**, 2902–2905.

149 A. Schoedel, W. Boyette, L. Wojtas, M. Eddaoudi and M. J. Zaworotko, *J. Am. Chem. Soc.*, 2013, **135**, 14016–14019.

150 D. Bradshaw, J. E. Warren and M. J. Rosseinsky, *Science*, 2007, **315**, 977–980.

151 X.-N. Cheng, W.-X. Zhang and X.-M. Chen, *J. Am. Chem. Soc.*, 2007, **129**, 15738–15739.

152 Y.-B. He, Z.-Y. Guo, S.-C. Xiang, Z.-J. Zhang, W. Zhou, F. R. Fronczek, S. Parkin, S. T. Hyde, M. O'Keeffe and B. Chen, *Inorg. Chem.*, 2013, **52**, 11580–11584.

153 D. Zhao, D. J. Timmons, D. Yuan and H.-C. Zhou, *Acc. Chem. Res.*, 2010, **44**, 123–133.

154 F. A. Paz, J. Klinowski, S. M. Vilela, J. P. Tome, J. A. Cavaleiro and J. Rocha, *Chem. Soc. Rev.*, 2012, **41**, 1088–1110.

155 M. M. Smulders, I. A. Riddell, C. Browne and J. R. Nitschke, *Chem. Soc. Rev.*, 2013, **42**, 1728–1754.

156 S. Jeong, D. Kim, X. Song, M. Choi, N. Park and M. S. Lah, *Chem. Mater.*, 2013, **25**, 1047–1054.

157 S. Jeong, D. Kim, S. Shin, M. D. Moon, S. J. Cho and M. S. Lah, *Chem. Mater.*, 2014, **26**, 1711–1719.

158 W. Bury, D. Fairen-Jimenez, M. B. Lalonde, R. Q. Snurr, O. K. Farha and J. T. Hupp, *Chem. Mater.*, 2013, **25**, 739–744.

159 R. Bagai and G. Christou, *Chem. Soc. Rev.*, 2009, **38**, 1011–1026.

160 M. M. Smulders, A. Jimenez and J. R. Nitschke, *Angew. Chem., Int. Ed.*, 2012, **51**, 6681–6685.

161 J. R. Nitschke, *Acc. Chem. Res.*, 2006, **40**, 103–112.

162 Y.-R. Zheng and P. J. Stang, *J. Am. Chem. Soc.*, 2009, **131**, 3487–3489.

163 Y.-R. Zheng, Z. Zhao, M. Wang, K. Ghosh, J. B. Pollock, T. R. Cook and P. J. Stang, *J. Am. Chem. Soc.*, 2010, **132**, 16873–16882.

164 W. Meng, T. K. Ronson, J. K. Clegg and J. R. Nitschke, *Angew. Chem., Int. Ed.*, 2013, **52**, 1017–1021.

165 B. J. Burnett, P. M. Barron, C. Hu and W. Choe, *J. Am. Chem. Soc.*, 2011, **133**, 9984–9987.

166 H. Chung, P. M. Barron, R. W. Novotny, H.-T. Son, C. Hu and W. Choe, *Cryst. Growth Des.*, 2009, **9**, 3327–3332.

167 E.-Y. Choi, P. M. Barron, R. W. Novotny, H.-T. Son, C. Hu and W. Choe, *Inorg. Chem.*, 2008, **48**, 426–428.

168 E.-Y. Choi, C. A. Wray, C. Hu and W. Choe, *CrystEngComm*, 2009, **11**, 553–555.

169 O. K. Farha, A. M. Shultz, A. A. Sarjeant, S. T. Nguyen and J. T. Hupp, *J. Am. Chem. Soc.*, 2011, **133**, 5652–5655.

170 S. Takaishi, E. J. DeMarco, M. J. Pellin, O. K. Farha and J. T. Hupp, *Chem. Sci.*, 2013, **4**, 1509–1513.

171 J. An, O. K. Farha, J. T. Hupp, E. Pohl, J. I. Yeh and N. L. Rosi, *Nat. Commun.*, 2012, **3**, 604–609.

172 T. Li, M. T. Kozlowski, E. A. Doud, M. N. Blakely and N. L. Rosi, *J. Am. Chem. Soc.*, 2013, **135**, 11688–11691.

173 H. Chun, D. N. Dybtsev, H. Kim and K. Kim, *Chem. – Eur. J.*, 2005, **11**, 3521–3529.

174 M. Kondo, S. Furukawa, K. Hirai and S. Kitagawa, *Angew. Chem., Int. Ed.*, 2010, **49**, 5327–5330.

175 S. S. Y. Chui, S. M. F. Lo, J. P. H. Charmant, A. G. Orpen and I. D. Williams, *Science*, 1999, **283**, 1148–1150.

176 Y.-Q. Tian, S.-Y. Yao, D. Gu, K.-H. Cui, D.-W. Guo, G. Zhang, Z.-X. Chen and D.-Y. Zhao, *Chem. – Eur. J.*, 2010, **16**, 1137–1141.

177 S. J. Garibay and S. M. Cohen, *Chem. Commun.*, 2010, **46**, 7700–7702.

178 T. Ahnfeldt, D. Gunzelmann, T. Loiseau, D. Hirsemann, J. r. Senker, G. Férey and N. Stock, *Inorg. Chem.*, 2009, **48**, 3057–3064.

179 X.-P. Zhou, Y. Wu and D. Li, *J. Am. Chem. Soc.*, 2013, **135**, 16062–16065.

This journal is © The Royal Society of Chemistry 2014

*Chem. Soc. Rev.*, 2014, **43**, 5952–5981 | 5979

180 W. Lu, D. Yuan, A. Yakovenko and H.-C. Zhou, *Chem. Commun.*, 2011, **47**, 4968–4970.

181 S. Sato, Y. Ishido and M. Fujita, *J. Am. Chem. Soc.*, 2009, **131**, 6064–6065.

182 J.-R. Li and H.-C. Zhou, *Nat. Chem.*, 2010, **2**, 893–898.

183 Y.-R. Zheng, W.-J. Lan, M. Wang, T. R. Cook and P. J. Stang, *J. Am. Chem. Soc.*, 2011, **133**, 17045–17055.

184 M. Eddaoudi, J. Kim, N. Rosi, D. Vodak, J. Wachter, M. O'Keeffe and O. M. Yaghi, *Science*, 2002, **295**, 469–472.

185 H. Deng, C. J. Doonan, H. Furukawa, R. B. Ferreira, J. Towne, C. B. Knobler, B. Wang and O. M. Yaghi, *Science*, 2010, **327**, 846–850.

186 Z. Zhang, W.-Y. Gao, L. Wojtas, S. Ma, M. Eddaoudi and M. J. Zaworotko, *Angew. Chem., Int. Ed.*, 2012, **51**, 9330–9334.

187 B. F. Hoskins and R. Robson, *J. Am. Chem. Soc.*, 1990, **112**, 1546–1554.

188 A. D. Burrows, *CrystEngComm*, 2011, **13**, 3623–3642.

189 A. D. Burrows, Post-synthetic Modification of MOFs, *Metal Organic Frameworks as Heterogeneous Catalysts*, RSC, UK, 2013 ch. 3.

190 M. J. Ingleson, J. P. Barrio, J. B. Guilbaud, Y. Z. Khimyak and M. J. Rosseinsky, *Chem. Commun.*, 2008, 2680–2682.

191 E. Dugan, Z. Wang, M. Okamura, A. Medina and S. M. Cohen, *Chem. Commun.*, 2008, 3366–3368.

192 Z. Wang and S. M. Cohen, *Angew. Chem., Int. Ed.*, 2008, **47**, 4699–4702.

193 D. Britt, C. Lee, F. J. Uribe-Romo, H. Furukawa and O. M. Yaghi, *Inorg. Chem.*, 2010, **49**, 6387–6389.

194 S. J. Garibay, Z. Wang, K. K. Tanabe and S. M. Cohen, *Inorg. Chem.*, 2009, **48**, 7341–7349.

195 S. J. Garibay, Z. Wang and S. M. Cohen, *Inorg. Chem.*, 2010, **49**, 8086–8091.

196 H. C. Kolb, M. G. Finn and K. B. Sharpless, *Angew. Chem., Int. Ed.*, 2001, **40**, 2004–2021.

197 T. Gadzikwa, G. Lu, C. L. Stern, S. R. Wilson, J. T. Hupp and S. T. Nguyen, *Chem. Commun.*, 2008, 5493–5495.

198 T. Gadzikwa, O. K. Farha, C. D. Malliakas, M. G. Kanatzidis, J. T. Hupp and S. T. Nguyen, *J. Am. Chem. Soc.*, 2009, **131**, 13613–13615.

199 M. Savonnet, D. Bazer-Bachi, N. Bats, J. Perez-Pellitero, E. Jeanneau, V. Lecocq, C. Pinel and D. Farrusseng, *J. Am. Chem. Soc.*, 2010, **132**, 4518–4519.

200 Y. Goto, H. Sato, S. Shinkai and K. Sada, *J. Am. Chem. Soc.*, 2008, **130**, 14354–14355.

201 H.-L. Jiang, D. Feng, T.-F. Liu, J.-R. Li and H.-C. Zhou, *J. Am. Chem. Soc.*, 2012, **134**, 14690–14693.

202 C.-D. Wu, A. Hu, L. Zhang and W. Lin, *J. Am. Chem. Soc.*, 2005, **127**, 8940–8941.

203 L. Ma, J. M. Falkowski, C. Abney and W. Lin, *Nat. Chem.*, 2010, **2**, 838–846.

204 E. D. Bloch, D. Britt, C. Lee, C. J. Doonan, F. J. Uribe-Romo, H. Furukawa, J. R. Long and O. M. Yaghi, *J. Am. Chem. Soc.*, 2010, **132**, 14382–14384.

205 M. Kawano and M. Fujita, *Coord. Chem. Rev.*, 2007, **251**, 2592–2605.

206 T. Kawamichi, T. Haneda, M. Kawano and M. Fujita, *Nature*, 2009, **461**, 633–635.

207 J. Marti-Rujas, N. Islam, D. Hashizume, F. Izumi, M. Fujita, H. J. Song, H. C. Choi and M. Kawano, *Angew. Chem., Int. Ed.*, 2011, **50**, 6105–6108.

208 T. K. Ronson, S. Zarra, S. P. Black and J. R. Nitschke, *Chem. Commun.*, 2013, **49**, 2476–2490.

209 Y.-B. Dong, Q. Zhang, L.-L. Liu, J.-P. Ma, B. Tang and R.-Q. Huang, *J. Am. Chem. Soc.*, 2007, **129**, 1514–1515.

210 Y. Inokuma, M. Kawano and M. Fujita, *Nat. Chem.*, 2011, **3**, 349–358.

211 M. Yoshizawa, J. K. Klosterman and M. Fujita, *Angew. Chem., Int. Ed.*, 2009, **48**, 3418–3438.

212 D. Fiedler, D. H. Leung, R. G. Bergman and K. N. Raymond, *Acc. Chem. Res.*, 2004, **38**, 349–358.

213 S. J. Dalgarno, N. P. Power and J. L. Atwood, *Coord. Chem. Rev.*, 2008, **252**, 825–841.

214 M. D. Pluth and K. N. Raymond, *Chem. Soc. Rev.*, 2007, **36**, 161–171.

215 K. Biradha and M. Fujita, *Angew. Chem., Int. Ed.*, 2002, **114**, 3542–3545.

216 O. Ohmori, M. Kawano and M. Fujita, *J. Am. Chem. Soc.*, 2004, **126**, 16292–16293.

217 Y. Inokuma, T. Arai and M. Fujita, *Nat. Chem.*, 2010, **2**, 780–783.

218 M. Fujita, D. Oguro, M. Miyazawa, H. Oka, K. Yamaguchi and K. Ogura, *Nature*, 1995, **378**, 469–471.

219 Y. Inokuma, S. Yoshioka, J. Ariyoshi, T. Arai, Y. Hitora, K. Takada, S. Matsunaga, K. Rissanen and M. Fujita, *Nature*, 2013, **495**, 461–466.

220 Q.-K. Liu, J.-P. Ma and Y.-B. Dong, *Chem. – Eur. J.*, 2009, **15**, 10364–10368.

221 Q.-K. Liu, J.-P. Ma and Y.-B. Dong, *J. Am. Chem. Soc.*, 2010, **132**, 7005–7017.

222 S. Horike, S. Shimomura and S. Kitagawa, *Nat. Chem.*, 2009, **1**, 695–704.

223 C.-D. Wu and W. Lin, *Angew. Chem., Int. Ed.*, 2005, **44**, 1958–1961.

224 I. H. Park, S. S. Lee and J. J. Vittal, *Chem. – Eur. J.*, 2013, **19**, 2695–2702.

225 G. Férey and C. Serre, *Chem. Soc. Rev.*, 2009, **38**, 1380–1399.

226 F. Millange, C. Serre, N. Guillou, G. Férey and R. I. Walton, *Angew. Chem., Int. Ed.*, 2008, **47**, 4100–4105.

227 J. An, S. J. Geib and N. L. Rosi, *J. Am. Chem. Soc.*, 2009, **131**, 8376–8377.

228 J. An and N. L. Rosi, *J. Am. Chem. Soc.*, 2010, **132**, 5578–5579.

229 J. An, C. M. Shade, D. A. Chengelis-Czegan, S. Petoud and N. L. Rosi, *J. Am. Chem. Soc.*, 2011, **133**, 1220–1223.

230 B. Li, Y. Zhang, D. Ma, T. Ma, Z. Shi and S. Ma, *J. Am. Chem. Soc.*, 2014, **136**, 1202–1205.

231 J. Yu, Y. Cui, C. Wu, Y. Yang, Z. Wang, M. O'Keeffe, B. Chen and G. Qian, *Angew. Chem., Int. Ed.*, 2012, **51**, 10542–10545.

232 J. Yu, Y. Cui, H. Xu, Y. Yang, Z. Wang, B. Chen and G. Qian, *Nat. Commun.*, 2013, **4**, 2719–2725.

233 Y. Liu, V. Kravtsov and M. Eddaoudi, *Angew. Chem., Int. Ed.*, 2008, **47**, 8446–8449.

5980 | *Chem. Soc. Rev.*, 2014, **43**, 5952–5981

This journal is © The Royal Society of Chemistry 2014

234 P. He, H. Liu, Y. Li, Z. Lei, S. Huang, P. Wang and H. Tian, *Mol. Simul.*, 2012, **38**, 72–83.

235 G. Calleja, J. A. Botas, M. Sánchez-Sánchez and M. G. Orcajo, *Int. J. Hydrogen Energy*, 2010, **35**, 9916–9923.

236 A. Blomqvist, C. M. Araujo, P. Srepusharawoot and R. Ahuja, *Proc. Natl. Acad. Sci. U. S. A.*, 2007, **104**, 20173–20176.

237 D. Himsl, D. Wallacher and M. Hartmann, *Angew. Chem., Int. Ed.*, 2009, **48**, 4639–4642.

238 K. L. Mulfort, O. K. Farha, C. L. Stern, A. A. Sarjeant and J. T. Hupp, *J. Am. Chem. Soc.*, 2009, **131**, 3866–3868.

239 S. S. Han and W. A. Goddard, *J. Am. Chem. Soc.*, 2007, **129**, 8422–8423.

240 P. Dalach, H. Frost, R. Q. Snurr and D. E. Ellis, *J. Phys. Chem. C*, 2008, **112**, 9278–9284.

241 S. Yang, X. Lin, A. J. Blake, G. S. Walker, P. Hubberstey, N. R. Champness and M. Schröder, *Nat. Chem.*, 2009, **1**, 487–493.

242 S. Yang, G. S. Martin, J. J. Titman, A. J. Blake, D. R. Allan, N. R. Champness and M. Schröder, *Inorg. Chem.*, 2011, **50**, 9374–9384.

243 J. Tian, L. V. Saraf, B. Schwenzer, S. M. Taylor, E. K. Brechin, J. Liu, S. J. Dalgarno and P. K. Thallapally, *J. Am. Chem. Soc.*, 2012, **134**, 9581–9584.

244 Q.-K. Liu, J.-P. Ma and Y.-B. Dong, *Chem. Commun.*, 2011, **47**, 7185–7187.

245 R. Custelcean, *Chem. Soc. Rev.*, 2014, **43**, 1813–1824.

246 S. R. Oliver, *Chem. Soc. Rev.*, 2009, **38**, 1868–1881.

247 H. Fei, L. Paw U, D. L. Rogow, M. R. Bresler, Y. A. Abdollahian and S. R. J. Oliver, *Chem. Mater.*, 2010, **22**, 2027–2032.

248 H. Fei, D. L. Rogow and S. R. J. Oliver, *J. Am. Chem. Soc.*, 2010, **132**, 7202–7209.

249 O. M. Yaghi and H. Li, *J. Am. Chem. Soc.*, 1996, **118**, 295–296.

250 H. Fei, M. R. Bresler and S. R. Oliver, *J. Am. Chem. Soc.*, 2011, **133**, 11110–11113.

251 D. L. Rogow, G. Zapeda, C. H. Swanson, X. Fan, A. G. Oliver and S. R. J. Oliver, *Chem. Mater.*, 2007, **19**, 4658–4662.

252 H. Fei, C. H. Pham and S. R. Oliver, *J. Am. Chem. Soc.*, 2012, **134**, 10729–10732.

253 X. Li, H. Xu, F. Kong and R. Wang, *Angew. Chem., Int. Ed.*, 2013, **52**, 13769–13773.

254 T. K. Maji, R. Matsuda and S. Kitagawa, *Nat. Mater.*, 2007, **6**, 142–148.

255 J. Fu, H. Li, Y. Mu, H. Hou and Y. Fan, *Chem. Commun.*, 2011, **47**, 5271–5273.

256 J.-P. Ma, Y. Yu and Y.-B. Dong, *Chem. Commun.*, 2012, **48**, 2946–2948.

This journal is © The Royal Society of Chemistry 2014

Chem. Soc. Rev., 2014, **43**, 5952–5981 | **5981**